This is a manuscript preprint submitted to EarthArXiv. This paper is under review for the Journal of the Geological Society of London. The authors welcome feedback on this article.

A new source-to-sink synthesis of the Middle Triassic Helsby Sandstone Formation (Sherwood Sandstone Group) river system of the British Isles

Abbreviated title: A new synthesis of Mid-Triassic rivers in Britain

Xiang Yan, Gary J. Hampson and Alexander C. Whittaker*

Department of Earth Science and Engineering, Imperial College London, London SW7 2AZ, UK

***Correspondence:** Xiang.yan19@imperial.ac.uk

XY: https://orcid.org/0009-0001-5167-3008

GJH: https://orcid.org/0000-0003-2047-8469

ACW: https://orcid.org/0000-0002-8781-7771

Abstract

Sediment grain size and mineralogy change in sediment routing systems from source to sink. A better understanding of sediment routing allows improved predictions to be made of the bulk grain-size and mineralogy of sandstone fairways. We present a new appraisal of sediment routing in the Triassic Helsby Sandstone Formation (Sherwood Sandstone Group) and lowermost Mercia Mudstone Group of the British Isles, which constitute a key play for geological sequestration of CO2. These strata were deposited and supplied by a major, north-flowing river system, which is traced from its source region in north France to beyond the Irish Sea. We construct a new, integrated litho- and chronostratigraphic model to correlate key units across the British Isles. We then present sediment isopachs and volumes for this chronostratigraphic interval, and resolve palaeogeographic discrepancies using published sedimentological datasets, supplemented by a new synthesis of bulk sandstone mineralogy. Finally, we present a unified, updated sediment routing map for the Helsby Sandstone Formation. Substantial north-south differences in bulk sandstone mineralogy indicate that that sediment input from tributaries modified the composition of the Helsby Sandstone Formation along the course of the sediment routing system.

Introduction

Sediment transport via rivers is a key surface process that transfers mass from sediment sources to sediment sinks. Source-to-sink systems can be divided into segments: areas of uplift and erosion where sediment is generated, areas of sediment bypass and transient storage, and subsiding depocentres (e.g. Somme et al., 2009; Romans and Graham, 2013; Helland-Hansen et al., 2016). The size, shape and distribution of sediment routing systems are controlled by their geomorphology (e.g. Somme et al., 2009; Helland-Hansen et al., 2016; Markwick, 2019), which is seldom completely preserved over deep time (Romans and Graham, 2013; Helland-Hansen et al., 2016). Consequently, reconstructing palaeogeography is essential for constraining source-to-sink sediment routing in the

46 geological record (e.g. Markwick, 2019; Wrobel-Daveau et al., 2022). Understanding source-
47 to-sink sediment routing is in turn a crucial tool to evaluate landscape responses to climate
48 change and tectonics, as well as for predictive resource exploration (Wrobel-Daveau et al.,
49 2022; Castelltort et al., 2023).

50 Source-to-sink sediment routing is commonly constrained by several methods, and
51 involves the integration of lithostratigraphy, chronostratigraphy, and palaeogeography, the
52 latter constrained by methods including quantitative provenance analysis, sedimentology and
53 palaeocurrents (e.g. Morton and Hallsworth, 1993; Hampson et al., 2014; Helland-Hansen et
54 al., 2016; Michael and Zuhlke, 2022; Castellort et al., 2023). Synthesising these data can
55 produce a defined stratigraphy and age model, sediment volumes, and a defined map of
56 sediment source areas and sinks.

57 The Triassic Sherwood Sandstone Group (SSG; **table 1**) of the British Isles represents
58 a regionally important, predominantly fluvial sediment routing system, dated c. 249-240 Ma
59 (**fig. 1a,** Hounslow and McIntosh, 2003; Hounslow and Gallois, 2023). The SSG was deposited
60 at low latitudes of ca. 20° N during the early breakup of Pangea (**fig. 1b**), and in the aftermath
61 of the Permo-Triassic extinction (Radley and Coram, 2016; Newell, 2017a; b). Much of the
62 SSG is interpreted to have been laid down by major, north-flowing river systems that originated
63 from Variscan highlands, now situated in northern France (**fig. 1c,** e.g. Wills, 1956; Burley,
64 1987; Tyrrell et al., 2012; Morton et al., 2016; Newell, 2017a; Burgess et al., 2025). The SSG
65 has served as a key target for hydrocarbon exploration and production (e.g. Cowan, 1993;
66 McKie et al., 1997, Floodpage et al., 2001; Medici et al., 2019a; Scorgie et al., 2021), for
67 geothermal energy production (Downing et al., 1983; Knox et al., 1984), and is a major
68 groundwater aquifer (Plant et al., 1999; Newell and Smith, 2009; Medici et al., 2019b). More
69 recently, the SSG has also become a key target for geological sequestration of CO_2 (e.g.
70 Holliday et al., 1991; Newell and Shariatipour, 2016; Scorgie et al., 2021; Chedburn et al.,
71 2022; English et al., 2024; Gibson-Poole et al., 2025; Head et al., 2025). During the mid-
72 Triassic, the SSG transitioned into the Mercia Mudstone Group (MMG), which forms the

sealfor the SSG reservoir (**fig. 1a**, e.g. McKie et al., 1997; Scorgie et al., 2021; Chedburn et al., 2022; English et al., 2024; Hounslow and Gallois, 2023).

The most recent holistic palaeogeography for this time interval, published more than 30 years ago (**fig. 1c,** Warrington and Ivimey-Cook, 1992), describes a major northward-directed sediment routing system originating from the remnant Variscan highlands of north France, flowing through a series of linked extensional basins in the British Isles, into the East Irish Sea Basin (EISB). This follows the older palaeogeographic interpretations from Wills (1970), Audley-Charles, (1970b), and Burley (1987). However, unlike previous interpretations, there is no mention or depiction of lateral sediment inputs, and sediment routing in the Wessex Basin and beyond the EISB remains unclear. Furthermore, the SSG-MMG transition is poorly understood. Finally, the palaeogeographic extent of the catchments which sourced the fluvial systems of the SSG remain poorly constrained, as is their relation to the wider palaeogeography of northwest Europe.

Integration of data and research that has become available since the publication of Warrington and Ivimey-Cook (1992) could help to address these knowledge gaps. For instance, subsequent regional studies on the British Triassic system have collected and synthesised existing information to build basin-scale depositional models (e.g. Hamblin et al., 1992; Jackson et al., 1995; Plant et al., 1999; Dunford et al., 2001; Newell, 2017b; 2023; Marsh et al., 2022) while quantitative provenance analysis (Tyrrell et al., 2012; Morton et al., 2013; 2016) has provided higher resolution constraints on sediment source areas and sediment routing within the SSG. At the same time, better characterisation of the pre-Triassic basement allows inferences to be made about source area composition (e.g. Baptiste, 2016; Butler, 2018). Emerging chronostratigraphy has allowed the improved correlation of coeval units both across the British Isles (Mange et al., 1999; 2007; Hounslow and McIntosh, 2003; Hounslow et al., 2017; Houslow and Gallois, 2023), and to the wider European Triassic system (Bourquin et al., 2011, McKie, 2017). Lastly, improved understanding of the early Triassic climate (Péron

et al., 2005; Ravidà et al., 2021) and tectonics (Newell, 2017a) have offered further insights into controls on sediment generation.

Consequently, the last 30 years of research has resulted in a situation in which the SSG and MMG of the British Isles is locally well-characterised in many aspects, yet is poorly resolved on the scale of the sediment routing system. The aim of this paper is to produce a comprehensive, up-to-date and quantitative reconstruction of this source-to-sink system, harmonised with the palaeogeography of northwest Europe. To this end, we develop a unified lithostratigraphic and chronostratigraphic synthesis of key units in the SSG and MMG, focussing on a well-defined chronostratigraphic interval consisting of the upper SSG and lower MMG, in which the sediment routing system is well constrained. We present new maps of the sediment fairway using standardised nomenclature compiled from previous palaeogeographic studies. Using these products as a framework, we present the first quantitative estimates of the volume and distribution of fluvial and aeolian deposits within the fairway. We then derive isopach maps and volumes for units of interestand we synthesise downsystem trends in sediment composition and provenance to characterise source-to-sink sediment routing, as well as the composition and extent of source areas. Ffinally, we use these data to evaluate the size and position of sediment inputs into the sediment routing system.

Geological framework

The British Triassic system begins during the lower Triassic with the SSG (Hounslow and McIntosh, 2003), and passes into the MMG during the mid-Triassic (**fig. 1a**, Hounslow and Gallois, 2023). Deposition occurred in a series of linked, N-S trending extensional basins throughout the British Isles, spanning the area between the English Channel and the Irish Sea (Warrington and Ivimey-Cook, 1992). Deposition occurred under an arid and semiarid climate, which is widely evidenced by sedimentology and palaeontology (e.g. Brookfield, 2008; Evans et al., 2011; McKie, 2014; Newell, 2017a; b; Coram et al., 2019).

The standardised lithostratigraphy of the SSG, defined by the British Geological Survey (BGS, Ambrose et al., 2014), divides the group into three formations based on a succession typified in the Cheshire Basin. These three standardised formations are the conglomeratic and sandy fluvial Chester Formation (CHF), the mixed fluvial-aeolian Wilmslow Sandstone Formation (WSF) and the fluvial-aeolian Helsby Sandstone Formation (HSF) (**fig. 2**; Ambrose et al., 2014; Newell, 2017a). Deposition of the HSF in the Wessex Basin and Worcester Graben was partially contemporaneous with the deposition of the lowermost MMG in the Cheshire Basin and EISB (**fig. 1a, c**). The stratigraphy of the MMG is similarly standardised (Howard et al., 2008), and is represented by the Tarporley Siltstone Formation (TSF) and the Sidmouth Mudstone Formation (SMF) (**fig. 2;** e.g. Warrington et al., 1970b; Wilson, 1990; 1993; Newell, 2017a).

The BGS standardised stratigraphy supersedes older stratigraphic terminology which differed between sedimentary basins (**fig. 2**). Unit names for basin-scale stratigraphy are presented in **Figure 2,** based on the synthesis of Ambrose et al. (2014) and Howard et al. (2008). Although the older, basin-scale terminology is still widely used (e.g. Newell, 2017a; b; Scorgie et al., 2021; Marsh et al., 2022; Chedburn et al., 2022), the standardised BGS stratigraphy enables the SSG and MMG to be represented effectively on the source-to-sink scale, as it allows units to be robustly correlated between basins whilst avoiding any complex or redundant terminology.

The CHF (**fig. 1a**) was laid down during the lower Triassic by a regionally significant fluvial system sourced from the remnant Variscan mountains in north France (e.g. Tyrrell et al., 2012; Morton et al., 2013; 2016). The system flowed northwards into the East Irish Sea Basin, possibly reaching Northern Ireland (Franklin et al., 2020; Moscardini et al., 2025). Deposition during the CHF occurred in a highly dynamic, but consistently hyperthermal semi-arid climate during the aftermath of the Permo-Triassic extinction (Sun et al., 2012), resulting in its unusually coarse grain size (Radley and Coram, 2016; Newell, 2017a).

The overlying WSF is conformable over the CHF **(figs. 1a, 2)**, and is interpreted to represent a period of dominantly aeolian activity caused by accelerated extensional faulting, resulting in the disconnection of basins and dissection of the SSG fairway (Newell, 2017a). The boundary between the WSF and the overlying HSF is largely unconformable (**fig. 2**), representing a period of tectonic uplift traditionally attributed to the Europe-wide Hardegsen tectonic event (Evans et al., 1993; Mange et al., 1999; 2007; Bourquin et al., 2011).

The HSF (**fig. 1a**) represents a second, mid-Triassic interval of fluvial activity (Newell, 2017a; b). The HSF was deposited in a more stable, albeit still semiarid climate (Newell, 2017a) coinciding with a biotic recovery (Benton and Spencer, 2002; Coram et al., 2019). The mid-Triassic then saw a gradual, diachronous aridification, with the river systems of the HSF retreating southwards. Fluvial-aeolian deposition was replaced by the playa lakes and marine evaporites of the MMG, initially in the EISB (**fig. 1a**, e.g. Greenwood and Habesch, 1991; Jackson et al., 1995; Plant et al., 1999; McKie, 2017) until fluvial activity finally ceased in the Wessex Basin, and the HSF was replaced by the MMG (Newell, 2017b; Hounslow and Gallois, 2023).

Deposition of the CHF and HSF has previously been attributed to the 'Budleighensis' River (sensu Wills, 1956; 1970; 1976). This was interpreted to be a regionally significant river system sourced from the Variscan massifs of northern France (Tyrrell et al., 2012; Morton et al., 2013; 2016) which flowed into EISB towards Ireland (e.g. Dunford et al., 2001; Franklin et al., 2020; Moscardini et al., 2025). The drainage scale of this fluvial system, approximately 1000km, would be comparable to the modern Ebro River in Spain (Helland-Hansen et al., 2016). Substantial changes in sediment mineralogy occur between the Wessex Basin and the East Irish Sea Basin (**fig. 1c,** Burley, 1987; Plant et al., 1999; Morton et al., 2013), and it remains unclear how important the northern France source area was for the sediment routing system, relative to other potential sediment inputs. In the CHF, it has been proposed that variations in clast concentration suggest substantial sediment inputs occurring downstream of the northern France source area (Burgess et al., 2025).

In the context of northwest Europe, the northern France source area is known as the Gallic Massif (sensu Sass et al., 2023), a major upland region encompassing the modern-day Variscan-Cadomian-aged Armorican Massif, the French Massif Central and the buried basement surrounding them, under the Paris Basin and English Channel. The north-flowing 'Budleighensis' system shared a Gallic Massif source area with two other substantial fluvial systems: an east-flowing system which deposited the Buntsandstein in France and Germany (the 'Alemania' river, *sensu* Ravidà et al., 2021), and a southeast-directed system which deposited the Buntsandstein in Iberia (e.g. Sanchez Martínez et al., 2012; Bourquin et al., 2011; McKie, 2017).

The SSG exists in tectonostratigraphic continuity with underlying Permian aeolian sandstones and playa lake mudstones, which represent the first significant basin fill after the extensional collapse of the Variscan Orogeny (e.g. Hamblin et al., 1992; Jackson et al., 1995; Newell, 2017a), as well as the overlying MMG (e.g. Howard et al., 2008; Hounslow et al., 2017; McKie, 2017). The post-depositional history of the SSG is variable between basins, however the unit has generally undergone 2-4 km of burial across the UK (e.g. Carter et al., 1995; Mikkelsen and Floodpage, 1997; Bray et al., 1998; Carter et al., 2001; Pharaoh et al., 2018). The northern section of the SSG fairway, particularly in northwest England and offshore in the Irish Sea, has additionally seen substantial exhumation and erosion during the Cenozoic, bringing the SSG to outcrop (e.g. Mikkelsen and Floodpage, 1997; Pharaoh et al., 2018).

Overall, four uncertainties remain in characterising the SSG of the British Isles, which this study addresses. First, the chronostratigraphy of the SSG and lower MMG is not rigorously integrated with the existing lithostratigraphy across the British Isles. Secondly, its sediment fairway and depositional volumetrics have not been mapped out or quantified. Third, variations in bulk sandstone mineralogy must be appraised down the sediment fairway. Finally, sediment routing, and source areas must be reappraised using updated, published data. We seek to address these research needs in this study.

Methods

A synthesis of the lithostratigraphy of the HSF, TSF and lower SMF was completed to allow for a correlation of units between sedimentary basins in the British Isles. Chronostratigraphy was synthesised using the magnetostratigraphically constrained section of the HSF in the Wessex Basin (Hounslow and McIntosh, 2003; Hounslow and Gallois, 2023), and an equivalent section in the EISB (Hounslow and McIntosh, 2003; Mange et al., 1999), which was then correlated to the global Triassic timescale (Ogg et al., 2020). These sections are then supplemented by published palynology, and the correlation of lithostratigraphic units and boundaries across the HSF, TSF and lower SMF. From this lithostratigraphic and chronostratigraphic model, a single, time-equivalent interval could then be defined across the British Isles as a basis for further spatial, volumetric and palaeogeographic analysis. This studied interval represents 5 Myr, from 246.5 Ma to 241.5 Ma, as detailed later.

To map the fairway of this chronostratigraphically defined interval, a geological database was compiled from published outcrop sections and borehole logs, and borehole records held by the BGS Onshore Single Borehole Index, the Bureau de Recherches Géologiques et Minières, the UK Onshore Geophysical Library, and the North Sea Transition Authority National Data Repository (n = 393). For data points where stratigraphic units were completely preserved and not truncated by erosion, unit thicknesses and dominant lithologies were recorded. Boreholes were also recorded where the defined stratigraphic interval was not deposited, delimiting the edge of the fairway (**fig. 3)**. In areas where data points were too dense to manually parse or where sources offered contradictory interpretations, published interpretations were prioritised. In the absence of any existing interpretations, original interpretations were made using wireline logs and lithological data. The sediment fairway was then mapped from these data. Where data were sparse or absent, or where the SSG was absent due to post-depositional erosion, the fairway was mapped based on existing geological constraints and palaeogeographic interpretations.

The resulting sediment fairway map was then integrated with nomenclature for sedimentary basins, palaeohighs and major structural features from existing palaeogeographic reconstructions (e.g. Wills, 1956; 1970, Audrey-Charles, 1970b; Burley, 1987; Warrington and Ivimey-Cook, 1992; Bourquin et al., 2011; Newell, 2017a) to create a full palaeogeographic framework for the middle Triassic of the British Isles. Our reconstruction addresses major unknowns in fairway extent and reconciles inconsistencies between previous interpretations.

Where the sediment fairway was sufficiently constrained by thickness data (**fig. 3**), stratigraphic thicknesses were combined with a series of points where deposition is inferred to be absent (n = 32), representing nondeposition around Triassic massifs from the previously developed palaeogeographic framework. These points were collectively interpolated with a regional fault map based on BGS data (DiGRock250k, 2008; 2013) and Newell (2017b) to produce isopach maps for each studied lithostratigraphic unit. From these isopach maps, resulting sedimentary rock volumes were then computed for each basin, and were converted to solid rock volumes by removing pore space, a parameter well-constrained by previous studies. For the HSF, we used porosity estimates compiled by Medici et al. (2019a) for the EISB, Cheshire, Midlands and Worcester basins **(table 2)**. Porosity for the Wessex Basin is estimated at 18% (**table 2,** Bowman et al., 1993; Newell and Shariatipour, 2016). The same value of porosity is assigned to both aeolian and fluvial deposits in the HSF in each basin. For the MMG, mean values of 14.9% for the TSF and 17.8% for the SMF (Parkes et al., 2021) were applied for all basins. The Preesall and Northwich Halites are assumed to have zero porosity.

Fluvial and aeolian HSF volumes were estimated from literature-derived basin-scale sedimentological trends. Previous basin-scale estimates of the proportion of fluvial deposits were calculated by Medici et al. (2019a), but were limited to outcrop observations and are therefore biased to basin margins. Furthermore, as their method of calculation is not explicit, it is challenging to verify these estimates. We provide new estimates for the proportion of fluvial

deposits based on basin-scale sedimentological trends derived from published outcrop, borehole and seismic data. Three depositional environments are recognised: fluvial, aeolian, and fluvial-aeolian. For each basin, these depositional environments are used to calculate the proportion of two deposit types: fluvial and aeolian. Fluvial depositional environments are considered to have a fluvial deposit content of 100%. Aeolian depositional environments are considered to have an aeolian deposit content of 100%. Fluvio-aeolian environments, where fluvial and aeolian strata coexist in close succession, are inferred to contain 50% fluvial deposits, and 50% aeolian deposits: the most probable, representative value. These derived proportions are then used to calculate the overall basin-scale volume of fluvial and aeolian deposits.

Petrographic data for bulk sandstone mineralogy in the HSF were compiled from 7 sources across 16 localities in the sediment fairway, resulting in 320 data points. These data cover both borehole and outcrop localities, and represent either fluvial or aeolian facies (Ali, 1982; Knox et al., 1984; Burley, 1987; Chisholm et al., 1988; Svendsen and Hartley, 2001; Scorgie et al., 2021; De Sainz Simpson, 2022; Meadows, pers. comms., see **supplementary material 2 for full dataset**). Owing to historical differences in point counting technique (e.g. Garzanti, 2019; Augustsson, 2021), these data cannot be compared as a single group but must be divided by method: Indiana and Gazzi-Dickinson, based on their classification of rock fragments (**see supplementary material 4 for more detail**). For each point counting method, data were grouped by basin, and then separated by aeolian and fluvial deposits to characterise the bulk mineralogical variability of sandstones within the sediment fairway. Sediment mineralogy within the HSF has also been studied in the context of quantitative provenance analysis (e.g. Plant et al., 1999; Tyrrell et al., 2012; Morton et al., 2013; 2016). These studies are equally important in constraining sediment routing and source areas, and are discussed separately in the basin-by-basin synthesis of sediment routing (see below).

Although the bulk mineralogy of the lower MMG has also been studied in its sand fraction (Scorgie et al., 2021; De Sainz Simpson et al., 2022) and silt-clay fraction (Jeans,

2006; Armitage et al., 2013; Jones et al., 2025), interpreting sediment routing in the MMG is problematic. There are no sediment provenance studies to support compositional data, and understanding of depositional environments in the MMG in the Cheshire Basin and EISB remains limited. For the purposes of this study, we hence focus on sediment mineralogy in the HSF. A first-order synthesis of diagenesis was then compiled to assess its impact on detrital mineralogy. This was then generalised throughout the fairway by using a compilation of burial histories for each basin. From this, the detrital mineralogy of the HSF in each basin could be characterised, and fairway-scale trends in bulk sandstone mineralogy in the HSF could be assessed.

Basin-level sedimentological data were then synthesised to reconstruct fairway sediment routing. Firstly, published, basin-scale studies characterising the HSF and lower MMG were collated. For each basin, previously documented palaeocurrents, sedimentological trends and quantitative provenance analysis results were catalogued. These datasets were further complemented by the new synthesis of bulk sandstone mineralogy, as well as the compilation of predominant lithologies from borehole logs (**fig. 3**). For each basin, a map of dominant lithofacies could then be created by plotting sedimentological trends and borehole lithological data within the previously established fairway limits. Sediment routing directions were determined from representative palaeocurrent indicators, basin-scale sedimentological trends and quantitative provenance analysis. Sediment inputs into the system were inferred using quantitative provenance analysis and our synthesis of bulk sandstone mineralogy. Where present, the degree of fluvial-aeolian interaction was also inferred from the synthesis of bulk sandstone mineralogy. Basin-level sediment routing was then linked together to provide a harmonised record of sediment routing within the whole fairway.

Using the previously developed palaeogeographic and sediment routing framework, emergent uplands across northwest Europe were then lithologically and, where possible, topographically characterised. Sediment routing for the HSF was then integrated with existing constraints on sediment routing in northeastern Iberia and northwest Europe to produce a

regionally consistent map of sediment sourcing. By constraining the extent and coverage of non-preserved drainage in the source areas of the HSF, the source-to-sink system could be further characterised.

Stratigraphy

Revised terminology

Table 1 lists of commonly abbreviated stratigraphic and geographic terms. The 'Budleighensis River' (sensu Wills, 1956) was conceived as the main, north-flowing river which brought the distinctive quartzite clasts of the CHF from a southern Variscan source area into the Midlands. Since then, the term 'Budleighensis' has expanded to encompass all fluvial activity occurring within the CHF and HSF (e.g. Plant et al., 1999; Tyrrell et al., 2012; Radley and Coram, 2016; Newell, 2017a; Franklin et al., 2020; Burgess et al., 2025). This is problematic, as the CHF and the HSF represent temporally and sedimentologically distinct river systems (e.g. Hounslow and McIntosh, 2003; Morton et al., 2013; Newell, 2017a). Further, multiple tributaries and bifurcations have been interpreted for these river systems (e.g. Smith and Edwards, 1991; Morton et al., 2016; Burgess et al., 2024; Gibson-Poole et al., 2025). Nomenclature which is more spatially generic but temporally rigorous is necessary to represent these source-to-sink systems. We henceforth refer to this system as a whole as the 'Sherwood River System', with the 'Sherwood-1 River System' referring to the rivers of the CHF, and the 'Sherwood-2 River System' referring to the rivers of the HSF.

We adopt the term Mid-Triassic Unconformity (*sensu* Newell, 2017a) for the early Anisian unconformity below the HSF (**fig. 4**). Its former name, the Hardegsen Unconformity (e.g. Ambrose et al., 2014), is misleading, as although likely caused by the same regional tectonic event, the Franco-German Hardegsen Unconformity is distinctly older than its British equivalent (Hounslow and McIntosh, 2003). The new terminology avoids any implied time equivalency between the two.

Lithostratigraphy

Our lithostratigraphic synthesis **(fig. 4)** builds on the standardised nomenclature in Howard et al. (2008) and Ambrose et al. (2014). The stratigraphy in **Figure. 4** is arranged by depocentre from south to north, i.e. down the depositional system. Basin-scale lithostratigraphic divisions are depicted to aid correlation, and to illustrate the spatio-temporal evolution of the SSG and MMG. Although the correlations of Howard et al. (2008) and Ambrose et al. (2014) terminate in the EISB and Solway Basin respectively, the SSG and lower MMG can be correlated further (e.g. Jackson et al., 1997; Mange et al., 1999; 2007; Simms, 2009) and we integrate these areas into our stratigraphic framework.

On the largest scale, the SSG is divided into four formations in accordance with Ambrose et al. (2014): the Hopwas Breccia Formation, the CHF, WSF, and HSF. The lower MMG, in accordance with Howard et al. (2008), is divided into the TSF and the SMF (**fig. 4**). The SSG overlies various Permo-Triassic units that represent the initial, post-Variscan basin fill.

The HSF represents the second period of fluvial activity within the SSG. In the western Wessex Basin, the HSF is divided into four well-characterised members at outcrop (**fig. 4**, Newell, 2017b). The HSF lies over a prominent ventifact horizon developed at the top of the CHF: a manifestation of the Mid-Triassic Unconformity (Hounslow and McIntosh, 2003). In the Central Wessex Basin, no formal lithostratigraphic divisions exist, though in the Wytch Farm oilfield, the HSF has previously been split into five units separated by widespread floodplain-playa deposits (McKie et al., 1997). In the Southampton 1 borehole, the HSF is divided into two members by lithology (Thomas and Holliday, 1982) and heavy mineral composition (**fig. 4,** Morton et al., 2016).

In the Worcester Graben, the HSF is divided into three members by lithology (**fig. 4**, Old et al., 1991; Barclay et al., 1997; Sumbler et al., 2000). The HSF here passes gradationally upwards and northwards into the TSF, which in turn grades into the SMF. The HSF remains

undivided in the Knowle, Needlewood, Hinkley and Stafford Basins of the Midlands, and similarly grades into the TSF and then the SMF (**fig. 4**).

The HSF is absent from the East Midlands Shelf. Instead, a ventifact horizon, marking the Mid-Triassic Unconformity, lies on top of the CHF (Burley, 1987; Newell, 2023). This is in turn overlain by the MMG, which has a well-defined stratigraphy in this area (Howard et al., 2008). It is argued that tectonic activity associated with the Mid-Triassic Unconformity uplifted the Pennine-Charnwood Ridge, preventing the Sherwood-2 river system flowing northeast (Warrington and Ivimey-Cook, 1992; Ambrose et al., 2014; Newell, 2017a; Newell, 2023). The East Midlands Shelf became reconnected to the Hinkley Basin during the late Anisian, towards the top of the studied interval (Ambrose et al., 2014; Jones et al., 2025).

In the Cheshire Basin, the HSF is typically divided into the fluvio-aeolian Thurstaston Member, the fluvial Delamere Member and the fluvio-aeolian Frodsham Member (**fig. 4;** Ambrose et al., 2014). It is likely that these members represent large-scale, interdigitating facies associations (Thompson, 1970a; Burley, 1987; Plant et al., 1999). In the northwest Cheshire Basin (**fig. 3**), the lower boundary of the HSF may lie at the base of the Delamere Member, with the previously identified Thurstaston Member being part of the WSF instead (Earp and Taylor, 1986; Hough, 2002). The HSF grades into the TSF, which locally contains the aeolian Malpas Sandstone Member (**fig. 4**; e.g. Plant et al., 1999; Wilson, 1993; Jackson et al., 1995; Mikkelsen and Floodpage, 1997). The TSF then grades into the SMF (Plant et al., 1999). The Northwich Halite Member lies within the SMF and forms a lithologically uniform marker unit across the basin (**fig. 4,** e.g. Evans and Holloway, 2005; Evans et al., 2011).

In the EISB, the Mid-Triassic Unconformity disappears (Jackson et al., 1995), and the HSF and WSF appear conformable (**fig. 4**). No accepted division of the HSF exists on a basin scale. The HSF has been variously divided into two or three members (Jackson et al., 1997). In the Morecambe Gas Field **(fig. 3)**, the HSF is split into four members, following the tripartite stratigraphy of the HSF in the Cheshire Basin with the addition of the Waterstones Member (Bushell, 1986). However, any stratigraphic equivalency implied by the assignment of

391 members is misleading, because these members represent large-scale, interdigitating facies
392 associations, as previously noted for the HSF in the Cheshire Basin (Meadows and Beach,
393 1993b). The isochronous and widespread 'Century Playa' interval, (**fig. 4**; Thompson and
394 Meadows, 1997; Meadows, 2006) is the only consistent, correlatable unit occurring within the
395 HSF. The top of the HSF is sharp with the overlying MMG. The TSF is only present in the
396 southeastern part of the EISB (Burley, 1987; Scorgie et al., 2021), with the SMF directly
397 overlying the HSF elsewhere **(fig. 4)**. The stratigraphic nomenclature of the MMG differs
398 between the offshore basin centre and onshore eastern basin margin, but strata in these
399 locations are directly correlatable. For example, the Preesall, Mythrop and Rossall Halites are
400 directly equivalent in both regions (**fig. 2, 4**). The Preesall Halite is also the lateral equivalent
401 of the Northwich Halite of the Cheshire Basin (**fig. 4;** Jackson et al., 1995; Howard et al., 2008).

402 In the Peel, Kish Bank and Central Irish Sea Basins, the Ormskirk Sandstone
403 Formation is equivalent to the HSF in the EISB (**fig. 4**, Mange et al., 1999; 2007; Floodpage
404 et al., 2001; Merlin Energy Resources Consortium, 2020). The Leyland Formation and
405 Preesall Halite of the MMG also correlate to their equivalents in the EISB (Chadwick et al.,
406 2001; Merlin Energy Resources Consortium, 2020). In the Solway Basin, the HSF is undivided
407 (**fig. 4**, Ambrose et al., 2014). The Silloth Halite is equivalent to the Preesall and Northwich
408 Halites in the EISB and Cheshire Basin (Jackson et al., 1995; Floodpage et al., 2001; **fig. 4**).

409 In the Larne Basin of Northern Ireland, HSF-equivalent units are absent, and instead
410 the siltstone-rich Lagavarra Formation (**fig. 4**) is present above the Mid-Triassic Unconformity
411 (e.g. Jackson et al., 1995; Simms, 2009). The Larne Halite of the SMF is likely correlative with
412 the Preesall and Northwich Halites of the EISB and Cheshire Basin, respectively (Jackson et
413 al., 1995).

414

415 ***Chronostratigraphy***

The base of the HSF, i.e. the Mid-Triassic Unconformity and its correlative conformities (**fig. 4**), is magnetostratigraphically dated to the lower Anisian in both the Wessex Basin and the EISB (Hounslow and McIntosh, 2003). This boundary is thus an approximately isochronous surface, at c. 246.5 Ma (Ogg et al., 2020).

The top of the HSF, i.e. the SSG-MMG boundary, is widely documented to become progressively older to the north (**fig. 4**). At the Devon Coast section in the Wessex Basin, this boundary is magnetostratigraphically dated to the lower Ladinian (Hounslow and Gallois, 2023), at c. 239.6 Ma (Ogg et al., 2020). In the Worcester Graben, palynology puts the upper part of the HSF within the Anisian or possibly the lower Ladinian, with the SMF being Ladinian in age. (**fig. 4**; Barclay et al., 1997). In the Midlands, palynology suggests the lower SMF is Anisian in age (**fig. 4**; Bridge and Hough, 2002). In the East Irish Sea Basin, magnetostratigraphy suggests the top of the HSF is mid-Anisian in age (lower Pelonsian, Hounslow and McIntosh, 2003), at c. 244 Ma (Ogg et al., 2020, **fig. 4**). On the East Midlands Shelf, the HSF is absent, though palynology suggests the TSF is Anisian in age (Howard et al., 2008).

Within the MMG of the Cheshire and East Irish Sea Basins, the Northwich and Preesall Halites (**fig. 4**) are interpreted to record marine transgressions (Greenwood and Habesch, 1991; Thompson and Meadows, 1997) and their top provides an isochronous surface of upper Anisian age (Jackson et al., 1995; Evans et al., 2011; Chedburn et al., 2022). The Anisian-Ladinian boundary (c. 241.5 Ma, Ogg et al., 2020) is constrained by palynology and lies just above this marker unit, within the upper Byley Mudstones in the Cheshire Basin and within the lower Kirkham Mudstones in the EISB (**fig. 4,** Wilson and Evans, 1990; Plant et al., 1999). The Silloth and Larne Halites in the Solway and Larne basins are thought to be correlative to the Preesall and Northwich Halites (Jackson et al., 1995), and therefore are of equivalent age (**fig. 4**).

From these chronostratigraphic constraints, a single, roughly time-equivalent interval, defined in duration by activity of the Sherwood-2 River System, can be projected along the

sediment routing system: Interval S2. The base of S2 (**fig. 4**, c. 246.5 Ma, Ogg et al., 2020) is taken at the Mid-Triassic Unconformity between the Wessex Basin and Cheshire Basin, and its correlative conformity (the HSF-WSF boundary) in the EISB, Solway Basin, Kish Bank Basin, Peel Basin and Central Irish Sea Basin **(fig. 4)**. In Northern Ireland, the base of S2 is taken as the unconformity at the base of the TSF. The top of Interval S2 follows the Anisian-Ladinian boundary (c. 241.5 Ma, Ogg et al., 2020) as closely as possible, but is defined separately for each basin. In the Wessex Basin, the top S2 boundary follows the HSF-SMF boundary, which is lower Ladinian in age (Hounslow and Gallois, 2023), c. 239.6 Ma (Ogg et al., 2020). The true Anisian-Ladinian boundary is within the upper Otterton Ledge Member of the HSF in the western Wessex Basin (Hounslow and Gallois, 2023), however the absence of correlation elsewhere in the Wessex Basin prevents this boundary from being used **(fig. 4)**. In the Worcester Graben, the Midlands and the East Midlands Shelf, we use the TSF-SMF boundary as the top S2 boundary. This boundary is roughly of Anisian-Ladinian age in the Worcester Graben. Although the boundary becomes older in the Midlands and the East Midlands Shelf, the absence of more distinctive stratigraphic markers within the SMF means the top of the TSF remains the best option for correlation **(fig. 4)**. In the Cheshire Basin, EISB and further north, the top of S2 is taken at the top of the Northwich and Preesall Halite Members of the SMF and their stratigraphic equivalents, which are late Anisian in age **(fig. 4)**.

In summary, Interval S2 encompasses the HSF, the TSF, and the SMF up to and including the Preesall and Northwich Halites and their stratigraphic equivalents. Interval S2 has a duration of approximately 5 Ma, but this may be longer in the Wessex Basin (c. 6.9 Ma), and shorter in the Midlands Basins (**fig. 4**). This time-defined stratigraphic interval serves as an important framework for sediment fairway mapping across the British Isles, subsequent volumetric calculations, and the creation of a temporally-defined sediment routing synthesis.

Palaeogeography and fairway extent

The mapped fairway of Interval S2 encompasses an area between the Wessex Basin in the south and the Central Irish Sea, Kish Bank and Peel Basins in the north, (**fig. 5**). The fairway is surrounded by major upland areas, and smaller, mostly non-emergent structural highs which separate basins.

The southernmost depocentre is the Wessex Basin, bounded by the Central English Channel High to the south, the Start-Cotentin High to the southwest, and the Cranborne-Fordingbridge High and Mendip High in the north (**fig. 5,** Newell, 2017a; b). While the Wessex Basin was previously considered a basin produced largely by E-W trending normal faults (e.g. Buchanan, 1998; Butler, 1998; Hawkes et al., 1998; Underhill and Stonely, 1998; Miliorizos and Ruffell, 1998), recent evidence suggests that Triassic extension was largely controlled by an older set of N-S extensional faults, consistent with the Triassic stress regime and structural configuration of the Wessex Basin (Newell, 2017b).

North of the Mendip High, the Wessex Basin passes into the Worcester Graben **(fig. 5)**. Although a connection between the two basins is critical in allowing long-distance, northwards sediment routing (Tyrrell et al., 2012; Newell, 2017a), there has been no consensus on the connection's location though the Mendip High (Audley-Charles, 1970; Wills, 1970; Burley, 1987; Warrington and Ivimey-Cook, 1992; Newell, 2017a; Burgess et al., 2025). We identify the point of connection in the area around the Shrewton 1 and Devizes 1 wells (**fig. 3**), which penetrate c. 70m of sandstone-siltstone facies, lithostratigraphically equivalent to the HSF. This area, termed the Pewsey Trough (PT, **fig. 5**), had been a N-S oriented, possibly fault-controlled depocentre since the Permian (Pullan and Donato, 2022), and persisted as a deep, distinct depocentre in the late Triassic during MMG deposition (Newell, 2024).

The Worcester Graben is, a structurally controlled depocentre controlled by the East Malvern Fault, the Inkberrow Fault and the Clopton-Clapton-Northleach Fault (**fig. 5,** Chadwick and Evans, 1995; Newell, 2017a), though the SSG also onlaps the pre-Permian basement to the west. There are four basins in the Midlands **(fig. 5)**, but they are grouped into

a single ‘Midlands Basins’ province in our source-to-sink synthesis, owing to their connectivity and small size. The Midlands Basins are joined across the Market Drayton Horst to the Cheshire Basin. This is a half-graben basin primarily bounded by the Wem-Red Rock Fault in the southeast (**fig. 5**), and is separated from the EISB by the Llyn-Rossendale Ridge (Plant et al., 1999). The EISB contains numerous N-S faults which split the basin into sub-basins (**fig. 5**, Jackson et al., 1995). Beyond the EISB, there are a series of smaller, fault-controlled depocentres, including the Solway, Larne, Peel, Kish Bank, Kingscourt and Central Irish Sea basins.

Lying to the east of the Pennine High is the East Midlands Shelf, a structurally simple, east-dipping ramp which forms the western edge of the Southern Permian Basin (McKie, 2017; Newell, 2023). The HSF is absent on the East Midlands Shelf, which was likely never a depocentre for this unit. If the HSF had been deposited here, the strata would need to have been removed by erosion after the Mid-Triassic Unconformity, yet the resulting unconformity has never been found in any basin. In line with existing interpretations, the East Midlands Shelf was separated from the main fairway by an emergent Pennine-Charnwood high (**fig. 5**, Warrington and Ivimey-Cook, 1992; Ambrose et al., 2014; Newell, 2017a; Newell, 2023), and only became reconnected to the Midlands Basins towards the end of this time interval (Ambrose et al., 2014; Jones et al., 2025).

Substantial upland areas likely served as sediment sources during the Triassic (e.g. Mange et al.,1999; 2007; Meadows, 2006; Tyrrell et al., 2012; Morton et al., 2013; 2016; Burgess et al., 2024). These include the Gallic Massif to the south of the Wessex Basin (**fig. 5,** sensu Sass et al., 2023). To the west, the SSG fairway is bounded by the Cornubian, Welsh and Irish Massifs, and to the east, by the Pennine High and London-Brabant Massif (**fig. 5**). Smaller elevated regions are also present within the sedimentary fairway: the South Staffordshire Horst and Coventry Horst in the Midlands, and the Isle of Man Massif and the Ogham Platform in the EISB (**fig. 5**).

Uncertainties in fairway extent

The southwesterly extent of the HSF in the Wessex Basin is largely unknown due to limited offshore exploration. The southernmost wells which penetrate the HSF are 97/12-1 (Ainsworth and Riley, 2010) and 97/24-1A (**fig. 3**). The southern limit for the sediment fairway can be plausibly constrained to lie between the southernmost Permo-Triassic seabed outcrop (**fig. 5**) and the modern-day Channel Islands and north France, a recognised sediment source for the SSG (Morton et al., 2013). The fairway extent in the rest of the Wessex Basin and Worcester Graben is constrained by well data, with mostly generally little postdepositional erosion (**fig. 5**).

North of the Worcester Graben, Interval S2 is only partially preserved following post-depositional erosion. Though existing palaeogeographic interpretations all agree that Triassic units had a greater distribution in the past, the interpreted extent to which they were formerly distributed varies (Wills, 1956; 1970; Audley-Charles, 1970; Warrington and Ivimey-Cook, 1992; Jackson et al., 1995; Dunford et al., 2001; Hounslow et al., 2006; Bourquin et al., 2011; McKie, 2017).

Multiple lines of evidence can be used to constrain the original depositional extent of Interval S2. The absence of basin margin deposits analogous to those in the Wessex Basin and Worcester Graben (e.g. Smith and Edwards, 1991; Barclay et al., 1997; Newell, 2017b), palaeocurrents directed across palaeohighs (e.g. Thompson et al., 1970b; Chisolm et al., 1988), outliers of SSG (Chisolm et al., 1988), and recycled Triassic detritus incorporated into younger deposits (Walsh et al., 1980; 2018) all indicate that the fairway extent used to be greater, and that the preserved distribution is primarily a reflection of where structurally-controlled basins were deepest (Chadwick and Evans, 1995). The most eroded area in the fairway encompasses the East Irish Sea, Peel, Kish Bank and Central Irish Sea Basins (**fig. 5**), which are interpreted to have formerly comprised a contiguous 'Greater Irish Sea Basin' (*sensu* Dunford et al., 2001; Meadows, 2006). However, we do not use this term as sediment routing west of the EISB remains poorly understood. The original sediment fairway can also be inferred from the extent of Permian sedimentation, which occurred under the same

extensional tectonic regime as the SSG. In the northern parts of the fairway, Interval S2 is likely to have overstepped, or at the very least equalled the distribution of Permian strata in the same way it does in the Wessex Basin and Worcester Graben, where both Permian units and the SSG are fully preserved (Hamblin et al., 1992; Chadwick and Evans, 1995). Our interpreted depositional boundaries (**fig. 5**) are conservative estimates based on these lines of evidence.

Sediment isopachs

Isopach maps, created from compiled data constraints (**fig. 5**), reconstruct deposited sediment thicknesses for Interval S2. Data coverage is sufficient to fully resolve sediment thicknesses between the Wessex Basin and the EISB (**fig. 6a**), and partially resolve thicknesses in the Solway and Peel basins north of the Ramsay-Whitehaven Ridge **(fig. 6a)**. These maps accurately resolve the spatial and structural configuration of the sediment fairway for the first time. Deposition of all lithostratigraphic units occurs in deep, structurally-controlled basins, with strata thinning over inter-basin palaeohighs (**fig. 6**). The East Midlands Shelf **(fig. 5)** was excluded from this volumetric analysis. As previously established, this was not a fluvial depocentre for the HSF, and stratigraphic markers coeval to those defining Interval S2 are absent (**fig. 4**, Howard et al., 2008).

The HSF in the Wessex Basin is thickest towards the west, at 320 m. The HSF thins gradually towards the east, and towards the Gallic Massif in the south (**fig. 6b**). Notably, thickness variations in the HSF are gradual **(fig. 6b)**, and appear only to be controlled by the oblique-slip Quantocks-Coker-Cranborne Fault System, which bounds the Cranborne-Fordingbridge High (**fig. 5, 6b,** Newell, 2017b). This shows that major W-E-trending extensional faults, which were active later in the Mesozoic (e.g. Buchanan, 1998; Butler, 1998; Hawkes et al., 1998; Underhill and Stonely, 1998; Miliorizos and Ruffell, 1998) were inactive in the Triassic. In the Worcester Graben, the HSF thickens westwards towards its faulted basin

margin, reaching a maximum of 400 m (**fig. 6b**), which represents the greatest depositional thickness along the fairway. In the Midlands, the maximum thickness of the HSF is approximately 220m in basin centres (**fig. 6b**). The HSF in the Cheshire Basin is thickest in the southeast, where thicknesses approach 210m (**fig. 6b**). Sediment thicknesses generally thin westwards towards the Llyn-Rossendale Ridge, and towards the southwestern basin margin. HSF thicknesses in the EISB are greatest at the basin centre, at 210m (**fig. 6b**), and decrease towards the basin margins.

The TSF is predominantly concentrated in the Cheshire Basin (**fig. 6c**), where thicknesses reach 200 m in the southeast. The TSF thins to the northwest towards the southeastern EISB. Here, thicknesses do not exceed 100m. To the south, the TSF is widely distributed but thin (<50 m) in the Midlands, East Midlands Shelf and the Worcester Graben, locally reaching 60 m thick in the hanging wall of the East Malvern Fault.

The lower SMF (below the Preesall and Northwich Halites) (**fig. 6d**) reaches up to 410 m thick in the northeastern Cheshire Basin, although it is generally 200-400 m thick elsewhere in the basin. In the EISB, the SMF gradually thickens towards the northwest part of the basin, where the unit reaches thicknesses of 900 m (**fig. 6d**). The SMF thins towards the Ramsay-Whitehaven Ridge, and the basin margin in the west.

The Northwich Halite in the Cheshire Basin reaches a maximum thickness of 230 m (**fig. 6e**), and is thickest along a NW-SE axis through the centre of the basin, thinning out towards the basin margins. The Preesall Halite is 570m thick in the centre of the EISB (**fig. 6e**), and is thickest along a N-S axis at the basin centre. Both the extent and the thickness of the Preesall Halite is reduced over the Llyn-Rossendale Ridge, where thicknesses do not exceed 200 m.

Sediment porosity and facies

601 The calculated proportion of aeolian and fluvial deposits reflects the distribution of
602 sediment at the time of deposition, and provides insight into the distribution of aeolian and
603 fluvial processes operating within the HSF fairway. It should be noted that this figure cannot
604 directly represent the extent of fluvial-aeolian sediment reworking, nor the ultimate provenance
605 of the sediments. These aspects require further sedimentological and petrographic data to
606 discern, and are discussed below as part of the basin-by-basin synthesis of sediment routing.

607 For the HSF, the proportion of fluvial deposits in the EISB is 64%, and was estimated
608 by averaging areas covered by mapped seismic facies (figs. 8 and 9 in Meadows and Beach,
609 1993b). The proportion of fluvial deposits in the Cheshire Basin is 71%, and was estimated
610 from vertical facies successions from borehole logs (figs. 6 and 7 in Thompson et al., 1970a).
611 In the Midlands and Worcester Graben, the composition of the HSF is assumed to be 100%
612 fluvial, as no widespread aeolian facies have been documented in outcrop, core or wireline
613 log data (Ambrose et al., 2014). In the Wessex basin, the first-order proportion of fluvial
614 deposits is estimated at 90% and is consistent in both the western and central areas (McKie
615 et al., 1997; Newell, 2017b).

616

617 ***Sediment volumes***

618 Solid rock (porosity removed) sediment volume for Interval S2 is 15,600 km³ (**fig. 7**,
619 with further data in **Supplementary Material 3**). Of this volume, 5,590 km³ (36%) is
620 represented by the HSF of the SSG. The remaining 10,000 km³ (64%) is represented by the
621 MMG. Within the MMG, 613 km³ is in the TSF, 6190 km³ in the lower SMF, and 3210 km³ in
622 the Preesall and Northwich Halites; these lithostratigraphic units comprise 4%, 40% and 20%
623 of the total sediment volume of Interval S2, respectively.

624 By volume, the EISB is the largest basin, with a total sediment volume of 9750 km³,
625 representing 62% of the total volume of Interval S2 (**fig. 7**). However, the HSF only comprises
626 1820 km³ (19%) of the EISB's sediment volume, and only 1160 km³ (12%) is composed of

627 HSF fluvial deposits. The Cheshire Basin is the second largest depocentre, with a total
628 sediment volume of 2500 km³. The HSF comprises 533 km³ (21%) of the Cheshire basin's
629 total volume, of which 379 km³ (15%) is fluvial deposits. The Wessex Basin is third largest
630 depocentre, with a total sediment volume of 1870 km³. Interval S2 is only composed of the
631 HSF here, with 1690 km³ of fluvial deposit volume. The Worcester Graben has a total sediment
632 volume of 1090 km³. Sediment volumes here are dominated by the entirely fluvial HSF, at
633 1030 km³ (95%). The remainder of this volume (54.5 km³, 5%) comprises the TSF. The
634 Midlands Basins are collectively the smallest depocentre, with a total sediment volume of 386
635 km³. Again, this volume is dominated by the entirely fluvial HSF, at 335 km³ (87%), with 51.7
636 km³ (13%) being the TSF. Overall, the largest volume of HSF occurs in the Wessex Basin,
637 followed by the EISB, the Worcester Graben, the Cheshire Basin, and then the Midlands
638 basins (**fig. 7**).

639 When sediment volumes are integrated with the well-constrained chronostratigraphy
640 in the EISB and Wessex Basin (**fig. 4**), solid rock sediment accumulation rates can be
641 calculated. In the EISB, Interval S2 has a total duration of 5 Ma: 2.5 Ma for the HSF, and 2.5
642 Ma for the lower MMG (TSF, SMF and Preesall Halite). In the Wessex Basin, Interval S2 has
643 a duration of 6.9 Ma. For the EISB, sediment accumulation rates increase fourfold from 726
644 km³/Myr in the HSF, to 3170 km³/Myr in the lower MMG. The overall accumulation rate across
645 Interval S2 in the EISB is 1950 km³/Myr. In the Wessex Basin, the sediment accumulation rate
646 within Interval S2 is 271 km³/Myr.

647

648 ***Errors and uncertainties in sediment volume***

649 Uncertainties in the original fairway extent cause uncertainties in calculated sediment
650 volumes. The greatest uncertainty in fairway extent occurs in the southwestern part of the
651 Wessex Basin, where there are very few constraints on the thickness and distribution of the
652 HSF (**fig. 3**). North of the Midlands (**fig. 6a**), uncertainties in fairway extent are caused by

post-depositional erosion. This uncertainty is reduced by the fact that basin centres are fully preserved and well-constrained, with only the former basin margins, where Interval S2 was thinnest, being eroded. Furthermore, as the boundaries of the sediment fairway are drawn from conservative estimates (**fig. 5**), the resulting isopach maps and sediment volumes are also conservative estimates.

Uncertainties in defining lithostratigraphic boundaries are low, as for most units, lithologies and wireline log responses are distinct (e.g. Meadows, 2006; Ambrose et al., 2014 Newell, 2017a; Chedburn et al., 2022). More uncertainty occurs in areas where the TSF is gradational between the HSF and the SMF. However, the impact of this uncertainty at the fairway scale is small, as the TSF is the volumetrically smallest unit in Interval S2 (**fig. 7**).

Uncertainty in rock porosity is generally low in the SSG, as porosity is well-characterised from a large dataset compiled across the sediment fairway (**Table 2**, Bowman et al., 1993; Newell and Shariatipour, 2016; Medici et al., 2019a). Uncertainties in the MMG are higher, as far fewer measurements of porosity are available (Parkes et al., 2021). However, owing to the limited range of porosities in mudstones (<20%, AlNajdi and Worden, 2023), the impact of porosity on sediment volume is limited compared to the other uncertainties discussed.

The classification of fluvial and aeolian deposits in the HSF in the Cheshire Basin and EISB represents a further uncertainty. Though there is good spatial coverage of basin-scale sedimentology, criteria used to recognise aeolian, fluvial and fluvial-aeolian successions differ between these basins (Thompson, 1970a; Meadows and Beach, 1993b). Our calculated fluvial and aeolian deposit volumes, which are derived from these facies distributions, represent a first-order estimation of the facies distribution within the sediment fairway.

Bulk sandstone mineralogy in the HSF

Data for bulk sandstone mineralogy in the HSF is outlined in table 3, and are classified by study, point counting method and depocentre. Overall, there is a notable difference in bulk sandstone mineralogy between the Wessex Basin in the southern part of the sediment fairway, and the Midlands basins, Cheshire Basin and EISB to the north (**fig. 8a**). Although there is an absence of data in the Worcester Graben, sandstones are clearly more feldspathic in the southern part of the fairway than the north (**fig. 8b,** see **Supplementary Material 4** for full dataset).

By the Gazzi-Dickinson method of point counting, quartz and feldspar are the dominant mineralogical components in the HSF, though proportions change substantially between basins. In the Wessex Basin, bulk sandstone mineralogy appears similar in both the eastern and western basin, with quartz, feldspar and lithic contents of 50-70%, 20-50% and 0-20%, respectively (**fig. 8b**; Knox et al., 1984; Hartley and Svendsen, 2001). Although there is no quantified petrographic data for the central part of the Wessex Basin (**fig. 8a)**, its bulk mineralogy appears comparable to the eastern and western Wessex Basin (Rhys, 1982; Bath et al., 1987). To the north, the HSF appears to have a similar bulk mineralogy in both the Cheshire Basin and EISB, with a quartz content of 80-95%, a feldspar content of 0-15%, and a lithic content of 0-10% (**fig. 8b**, De Sainz Simpson, 2022). Furthermore, fluvial and aeolian sandstone facies in the Cheshire Basin and EISB appear to have a similar bulk mineralogy.

By the Indiana method of point counting, resultant proportions of quartz, feldspar and lithic fragments are more variable, though again, mineralogical proportions vary between basins. In the Wessex Basin, the HSF largely has a quartz content is of 40-70%, a feldspar content of 15-50%, and lithic content of 10-50% (**fig. 8a,** Burley et al., 1987). In the Cheshire Basin and EISB, bulk sandstone compositions are similar, with quartz, feldspar and lithic contents of 50-90%, 0-25%, and 5-40%, respectively (**fig. 8b;** Burley, 1987; Scorgie et al., 2021; Meadows, pers. comm). In the Cheshire Basin, there appears to be a difference in bulk mineralogy between fluvial and aeolian facies, with aeolian sandstones (n = 4) being more

quartz-rich than fluvial sandstones (n = 58). In the EISB, fluvial and aeolian facies appear to have a similar bulk mineralogy.

Sediment mineralogical data appear consistent in the Midlands, despite the point counting method being unclassified. The quartz content of sandstones is 80-90%, the feldspar content is 5-15%, and the lithic content is 2-10% (**fig. 8b,** Ali, 1982; Chisholm et al., 1988).

Diagenesis and its impact on bulk sandstone mineralogy

Diagenetic alteration of unstable detrital grains also contributes to uncertainties in reconstructing original bulk sandstone mineralogy. Lithic fragments and feldspars are ubiquitously altered in the HSF across all basins, evidenced by grain dissolution textures, skeletal grains, and the presence of authigenic clays and feldspars (e.g. Ali and Turner, 1982; Burley, 1984; Knox et al., 1984; Bushell, 1986; Strong and Milodowski, 1987; Greenwood and Habesch, 1993; Plant et al., 1999; Scorgie et al., 2021). Grain dissolution porosity is measured at 7% in Devon in the western Wessex Basin, 8% in the Marchwood 1 borehole in the eastern Wessex Basin, and up to 7% in the EISB margin (Burley, 1984).

On the fairway scale, the maximum burial depth for the HSF can be used to approximate the maximum effects of diagenesis in each basin. The burial histories for each basin (**fig. 9**) are derived from apatite fission track analysis and vitrinite reflectance (Carter et al., 1995; Mikkelsen and Floodpage, 1997; Bray et al., 1998; Gent, 2006; Pharaoh et al., 2018). Selected wells are located away from basin margins, and so likely represent maximum burial depths for each respective basin. The burial depth for the HSF at the Wytch Farm oilfield in the Wessex Basin is 3.5 km (Bray et al., 1998). The SSG in the Midlands Basins reached a palaeotemperature of 75 ± 10 °C between 150 and 70 Ma (Carter et al., 1995). Assuming a geothermal gradient of 30 °C/km, this implies a burial depth of 2.5 ± 0.3 km (**fig. 9b**). The HSF in the Knutsford 1 well in the Cheshire Basin reached a burial depth of 2.9 km (**fig. 9b**, Mikkelsen and Floodpage, 1997), and for well 110/7b-6 in the EISB, 1.8 km (**fig. 9b,** Gent,

2006; Pharaoh et al., 2018). This implies the HSF across Great Britain reached comparable maximum burial depths (c. 3km), except in the EISB, which was buried to shallower depths (c. 2km). This in turn suggests that the maximum impact of diagenesis is relatively similar in all basins except for the ESIB, which may have experienced less extreme diagenetic alteration.

These figures indicate that HSF sandstones were originally more lithic- and feldspar-rich, with a modest amount (<10% total rock volume) of grains removed during burial diagenesis. Data points in **Figure 8b** cannot be translated uniformly to remove diagenetic effects, as burial depths and diagenetic histories differ for data collected at basin margins and palaeohighs, compared to deeper basin centres (Green et al., 1995; Bray et al., 1998; Scorgie et al., 2021). However, the variance of bulk sandstone detrital mineralogy both within basins and between basins **(fig. 8b)** is substantially greater than any compositional variations expected from diagenesis. This in turn indicates that spatial variations in sandstone composition are a primarily depositional signal, and so can be used to interpret sediment routing within the fairway.

Fairway sediment routing

Overall, our source-to-sink synthesis suggests Interval S2 was deposited by a single, continuous fluvial system, evidenced by consistently north and northwest-directed palaeocurrents and an overall decrease in grain size along the sediment fairway **(fig. 10a, b).** The connectivity of sediment routing is also strongly supported by our synthesis of quantitative provenance analysis (Plant et al., 1999; Tyrrell et al., 2012). Our synthesis also resolves the presence of secondary sediment inputs and fluvial-aeolian interactions, and provide insight into sediment routing beyond the EISB and across the transition between the SSG and MMG (i.e. the distal segments of the Sherwood-2 River System). A more detailed overview of sediment routing in the Wessex, Cheshire and East Irish Sea Basins, as well as the SSG-

MMG transition, is presented in **Supplementary Material 5** to honour the breadth and depth of published information available.

Sediment routing within the HSF

In the Wessex Basin, quantitative provenance analysis indicates the Sherwood-2 River System operated as a series of at least three north-flowing tributaries (**fig. 10a,** Morton et al., 2016). The HSF is dominated by material with a Variscan-Cadomian provenance, sourced from the basement units of the Gallic Massif (Tyrrell et al., 2012; Morton et al., 2013; 2016). This is supplemented by material sourced from the granites of the Cornubian Massif (Smith and Edwards, 1991) and recycled Devonian sediment from the London-Brabant Massif (Morton et al., 2016). All tributaries likely coalesced south of the Pewsey Trough and flowed nothwards as a single trunk river into the Worcester Graben **(fig. 10a)**.

In the Worcester Graben, the main axis of sediment routing was to the north (**fig. 10a,** Old et al., 1991). Although the presence of extraformational clasts in the HSF suggest proximal sediment inputs (Barclay et al., 1997; Old et al., 1999), there are no contemporary studies of sediment provenance or petrography in the Worcester Graben, and the details of sediment routing here are largely unknown.

In the Midlands Basins, recorded palaeocurrent azimuths suggest the primary axis of sediment routing was northwards (**fig. 10a,** Old et al., 1987; 1991, Chisolm et al., 1988). Multiple sediment inputs from the Welsh and London-Brabant Massifs are proposed by Audley-Charles (1970), based on observed clast compositions in the HSF (**fig. 10a**). The pronounced difference in HSF bulk sandstone composition between the Wessex Basin and the Midlands basins (**fig. 8b**) suggests that substantial dilution of Variscan-derived material by sediments from other source areas had already occurred before the Sherwood-2 River System reached the Midlands Basins (Plant et al., 1999; Morton et al., 2013). However, bulk sandstone mineralogical data for the Midlands Basins is limited (**fig. 8b**), and thus the mineralogical diversity of the HSF here may not be fully captured. The CHF in the Midlands appears to have

782 a substantial lithic component (Indiana method, Burley, 1986) which could also be present in
783 the HSF.

784 During much of Interval S2, an emergent Pennine-Charnwood Ridge disconnected the
785 Sherwood-2 River System from the East Midlands Shelf. Accordingly, the East Midlands Shelf
786 was devoid of large-scale fluvial activity, and was instead a low-energy coastal plain where
787 the MMG was deposited (Jones et al., 2025). Reconnection between the Midlands and the
788 East Midlands Shelf occurred during the latter stages of Interval S2 during deposition of the
789 TSF **(fig. 10b)**.

790 In the Cheshire Basin, palaeocurrents suggest the main axis of fluvial transport was
791 towards the northwest (**fig. 10a,** Thompson, 1970b; Plant et al., 1999; Mountney and
792 Thompson, 2002; De Sainz Simpson, 2022; Cosgrove et al., 2025). This was accompanied
793 by input of fluvial sediment from the Welsh Massif (Plant et al., 1999) (**fig. 8b**). A further, well-
794 documented component of aeolian activity is associated with the fluvial system. Palaeowinds
795 originated from the east, and aeolian sediment was sourced from the Pennine High (**fig. 10a**,
796 Thompson, 1970b; Rees and Wilson, 1998; Mountney and Thompson, 2002; De Sainz
797 Simpson, 2022; Cosgrove et al., 2025). The proportion of fluvial and aeolian deposits is highly
798 variable both spatially and temporally (e.g. Burley, 1987; Cosgrove et al., 2025), and their
799 distribution likely had underlying climate and subsidence controls, which in turn controlled
800 sediment flux, accommodation generation, and water table level (Newell, 2017a; Cosgrove et
801 al., 2025). In spite of this variability, a throughgoing, northwest-flowing fluvial system was
802 maintained, as widespread, perennial fluvial activity occurred downsystem in the EISB
803 (Meadows and Beach, 1993a; b; Meadows, 2006).

804 In the EISB, the Sherwood-2 River System entered the basin in the south, and then
805 turned west (Cowan, 1993; Herries and Cowan, 1997; Plant et al., 1999; Dunford et al., 2001;
806 Meadows, 2006; Marsh et al., 2022). Here, Mange et al. (1999, 2007) also identifies a
807 sediment input from the Welsh Massif **(fig. 10a)**, though this signal may have propagated from
808 the Cheshire Basin. There was also an aeolian sediment source from the Pennine High to the

east (**fig. 10a,** Meadows and Beach, 1993a; Jones and Ambrose, 1994; Meadows, 2006; Scorgie et al., 2021; Marsh et al., 2022). There was likely considerable aeolian reworking of fluvial sediments in the EISB prior to deposition: monocrystalline feldspars within both fluvial and aeolian facies have a provenance signal suggesting a Gallic Massif source (Tyrrell et al., 2012). There is no systematic variation in mineralogy between facies (**fig. 8b**) suggesting that these feldspars were also well-mixed in the basin. The provenance of the lithic fragments, which are composed primarily of quartz and feldspar and are also present in the Cheshire Basin (**fig. 8b**), is currently unknown. More marginal localities of the EISB are 100% aeolian (Jones and Ambrose, 1994; Medici et al., 2019a), whereas major fluvial activity is maintained in the basin centre, with aeolian facies only comprising 5-10% of the rock volume in the Morecambe gas field (Cowan, 1993). In more detail, spatial partitioning of fluvial and aeolian deposits in the basin may have followed structurally controlled highs and lows (Meadows and Beach, 1993b).

After the EISB, the Sherwood-2 River System flowed further west to the Kish Bank, Peel, and Central Irish Sea basins. These basins formerly formed a contiguous depocentre with the EISB (**fig. 10a,** Dunford et al., 2001; Meadows, 2006; Marsh et al., 2022). The sedimentology of the HSF in these basins is poorly characterised relative to the rest of the HSF fairway, a problem exacerbated by the severe degree of post-Triassic erosion in the area. All basins contain a mix of fluvial and aeolian sandstone facies (Newman, 1991; Naylor et al., 1993; Dunford et al., 2001; Floodpage et al., 2001).

During the early stages of Interval S2, the Irish Sea area was unlikely to have been the ultimate terminus of the Sherwood-2 River System, as there is no indication of an endorheic terminal splay system here (e.g. McKie, 2011; 2014, Gibson-Poole et al., 2025). Topographic barriers, and an absence of fluvial facies within strata equivalent to Interval S2 indicate the Sherwood-2 River System did not flow north towards the Solway and North Channel basins (**fig. 10a,** Marsh et al., 2022) or south into the Celtic Sea Trough (**fig. 10a**, Dunford et al., 2001). It is most likely that the Sherwood-2 River System therefore flowed west via the

836 Kingscourt Basin, possibly draining externally towards the shallow marine Porcupine Basin,
837 west of Ireland (Croker and Shannon, 1987).

838

839 ***Sediment routing across the SSG-MMG transition***

840 The onset of MMG deposition is diachronous (**fig. 4**), and coincides with the regional
841 Muschelkalk marine transgression and a climatic aridification (Greenwood and Habesch, 1991;
842 Thompson and Meadows, 1997; McKie, 2014; Newell, 2017a). Within the lower MMG, marine
843 flooding was brief, shallow but regular, and is well-evidenced through isotope geochemistry,
844 sedimentology and palaeontology (e.g. Greenwood and Habesch, 1991; Old et al., 1991;
845 Thompson and Meadows, 1997; Barclay et al., 1997; Evans, 2011; Warrington and Pollard,
846 2021). These transgressions likely originated from the marine domain west of Ireland (Croker
847 and Shannon, 1987) and combined with aridification, caused a southwards backstepping of
848 fluvial activity and an ingress of halite lake and playa facies initially into the EISB, but then into
849 the Cheshire Basin, Midlands basins and Worcester Graben by the end of the Anisian (**fig. 4,**
850 **10b**).

851 In the EISB, there is a sharp transition from the aeolian and sabkha deposits of the
852 HSF into the playa lake deposits of the SMF (**fig. 4**, Thompson and Meadows, 1997; Meadows,
853 2006). In the Cheshire Basin, the aeolian-dominated upper HSF transitions into the playa
854 margin deposits of the TSF (**fig. 4; 6c;** Mikkelsen and Floodpage, 1989; Burley, 1987; Scorgie
855 et al., 2021; De Sainz Simpson, 2022). In the Midlands Basins and Worcester Graben, the
856 fluvial deposits of the HSF transition into fluvial, playa margin and marginal marine deposits
857 of the TSF (e.g. Warrington, 1970a; b; Charsley, 1982; Old et al., 1991; Barclay et al., 1997;
858 Warrington and Pollard, 2021; Jones et al., 2025), although these latter successions are thin
859 and impersistent (**fig. 6c**). The Worcester Graben represents the southern limit of marginal
860 marine deposits in the TSF (**fig. 4**). In the Wessex Basin, the uppermost HSF is composed of
861 ephemeral lacustrine and sandflat deposits in the basin centre (McKie et al., 1997), and is

fluvial in the west (Newell, 2017b). Both areas then transition into the arid playa lake mudstones of the SMF **(fig. 4)**. Although sand-grade sedimentation ceased during the deposition of the MMG, the dominance of terrestrial and shallow subaqueous depositional environments in this unit (Arthurton 1980; Wilson, 1993) imply sediment fluxes remained sufficient to fill basins. The EISB was filled despite the previously calculated fourfold increase in sediment accumulation rate across the SSG-MMG boundary. A general increase in accommodation generation through time, due to varying tectonic subsidence rate (Newell, 2017a), may have contributed to the southwards retreat of sand-grade deposition (e.g. Paola and Martin, 2012; Reynolds, 2024). Further insight into the role of active faulting in controlling stratigraphic architecture is only possible with decompaction and better chronostratigraphic constraints.

During the later stages of Interval S2, the assemblage of evaporitic playa lake, playa margin, and intercalated fluvial-aeolian deposits in the SMF, TSF and HSF (**fig. 4**) corresponds well to a terminal splay depositional model (e.g. Lang et al., 2004; McKie, 2011, 2014). Incoming fluvial systems were dispersed at the playa margin. Fluvial activity became increasingly ephemeral and unconfined, and declined rapidly towards the basin-centre playa lake (**fig. 10b**). The SSG-MMG transition therefore represents the southward retreat of the Sherwood-2 River System. The absence of fluvial facies in the upper HSF and TSF in the EISB and Cheshire Basin may be due to preservational bias, as inactive fluvial deposits were rapidly reworked and incorporated into playa margin and aeolian deposits (Lang et al., 2004; McKie, 2011).

In the EISB and Cheshire Basin, the large volumes of SMF observed **(figs. 4, 6d, e)** were deposited in ephemeral lacustrine and dry mudflat settings (Arthurton, 1980; Wilson, 1990; 1993). The provenance of the MMG has not been directly addressed in this part of the British Isles. Ephemeral lacustrine sediments were likely sourced from distal flash floods, of which the Sherwood-2 River System would have been a contributor. Dry mudflat deposits require fine sediments with an aeolian source. In modern arid settings, fine sediments are

highly mobile, and can be transported for hundreds of kilometres by dust storms (Jefferson et al., 1990; Brookfield, 2008; McKie, 2011; Mao et al., 2021; Marx et al., 2022). While the nature of lacustrine-aeolian reworking, as well as preservational biases within playa settings, require further study (McKie, 2011), it is probable that not all the mudstone within the SMF has an origin from the Sherwood-2 River System. West-blowing Triassic palaeowinds may have served to rework sediment both into, within and out of these basins (**fig. 10b**).

Source areas and regional correlation of the Sherwood-2 River System

Palaeo-lithological domains

Upland areas of pre-Triassic bedrock represent the ultimate source of sediment for the Sherwood-2 River System (**fig. 11**). The pre-Triassic surface of northwestern Europe is lithologically diverse, and encompasses an area from the core of the Variscan Orogeny in the south (Baptiste, 2016; Martínez Catalán et al., 2021) to the Palaeozoic sedimentary cover of cratonic Avalonia in the north (Butler, 2018).

Although the distribution of basement lithologies during the Triassic is not known, key Variscan basement units had already been exhumed and were supplying sediment to the British Isles by the end of the Carboniferous (c. 300 Ma, Hallsworth et al., 2000; Jones et al., 2011; Morton et al., 2021; 2024). The pre-Triassic geology of northwest Europe can be categorised by large-scale tectonic domains, each with a differing geological history resulting in a distinct metamorphic, igneous and sedimentary succession. Domains have been characterised using outcropping lithologies, and in places where the pre-Triassic surface is buried under more recent sedimentary cover, using boreholes and geophysical methods (Baptiste, 2016; Butler, 2018). Where possible, we focus on the distribution of granitoids and gneisses, which provide provenance-sensitive feldspars, zircons and other heavy minerals to their respective fluvial catchments (Paul et al., 2008; Sanchez Martínez et al., 2012; Tyrrell et

al., 2012; Morton et al., 2013; 2016; Augustsson et al., 2018; Sass et al., 2023). Additional constraints on sediment routing, including inferences made from known constraints on palaeotopography, can be found in **Supplementary Material 5.**

Internal Variscan metamorphic units

The internal Variscan metamorphic units comprise a complex sequence of tectonic domains, which form the core of the Variscan Orogen in northwest Europe. The Mid-Variscan Allochthon forms much of the basement in central France (**fig. 11**). Variscan-aged granitoids, gneisses and migmatites are found throughout this unit, and are presently the most common group of rocks (Baptiste, 2016; Catalán et al., 2021). The North and Central Armorican tectonic domains to the north are primarily composed of metasediments and, respectively, Cadomian-aged granitoids and gneisses and Varican granites (**fig. 11,** Baptiste, 2016). The northernmost tectonic domain is the Léon-Normannian-Saxothuringian Domain, which lies mostly at subcrop and under the English Channel in the study area, and is poorly characterised (Shail and Leveridge, 2006). However, in north Brittany, this domain contains Variscan granitoids (Catalán et al., 2021). In the east, this domain also contains Cadomian granitoids or gneisses, and the Variscan Barfleur Granite (Baptiste, 2016; Donato et al., 2023).

The Gallic Massif is entirely composed of internal Variscan metamorphic units. (**fig. 10a, 11**). In the Wessex Basin, the delivery of Variscan-aged feldspars to the HSF necessitates a sediment source in the Central Armorican Zone and Mid-Variscan Allochthon, where the closest Variscan granitoids are concentrated. This yields approximately 300 km of non-preserved drainage for the Sherwood-2 River System over the Gallic Massif (**fig. 11**). In the central and eastern Wessex Basin, observed Variscan ages (Morton et al., 2016) are likely derived from the Barfleur Granite in northern France, owing to its proximity to the sediment fairway **(fig. 11)**. In southern Brittany, the Biscay Rift likely directed fluvial systems south towards the Iberian Peninsula (**fig. 11**, Péron et al., 2005; Bourquin et al., 2011; Sanchez

Martínez et al., 2012). The remaining part of the Gallic Massif is inferred to have supplied the Franco-German Buntsandstein **(fig. 11)**. This configuration allows for Cadomian and Variscan source signals to be supplied to this latter sediment routing system (Paul et al., 2008; Augustsson et al., 2018; Sass et al., 2023).

Dominantly sedimentary domains

Two basement tectonic domains are predominantly composed of sedimentary rocks: the Rhenohercynian Zone , which represents the Variscan fold-and-thrust belt, and Cratonic Avalonia, which has experienced mild to no Variscan deformation **(fig. 11)**. Both domains are both composed of synorogenic Variscan clastic sediments, as well as carbonates and clastics predating the Variscan Orogeny (e.g. Busby and Smith, 2001; Butler, 2018; Pharaoh, 2021). The Rhenohercynian Zone additionally hosts Variscan granites of the Cornubian Batholith, with an associated contact metamorphic aureole (**fig. 11,** Searle et al., 2024). In the Triassic the Rhenohercynian Zone and Cratonic Avalonia would have had a more extensive cover of younger and stratigraphically higher Carboniferous rocks, since removed by erosion.

The catchment for the Sherwood-2 River System likely extended into the Cornubian Batholith in the RHZ, around 30 km west of the Wessex Basin (**fig. 4**) (Smith and Edwards, 1991; Morton et al., 2013). On the eastern side of the Wessex Basin, the London-Brabant Massif lies in both the RHZ and Cratonic Avalonia, and has potential to provide a sizeable drainage area into the S2 fairway. However, the extent of the drainage which supplied recycled Devonian clastics from the London-Brabant Massif (Morton et al., 2016) is unclear owing to the large areal extent of this source, and the abundant subcrop of this lithology beneath the Variscan unconformity (Butler et al., 2018). The Welsh Massif also has potential to supply a sizeable drainage area for the S2 fairway (**fig. 10a**), and HSF sandstones in the EISB appear to have been derived from North Wales (Mange et al., 1999), though the overall extent of this catchment remains unclear. The Pennine High separates the mudstone-dominated East Midlands Shelf from the sandstone-dominated EISB, and was a well-documented sediment

source for the latter (Meadows and Beach, 1993a; Meadows, 2006; Scorgie et al., 2021; Marsh et al., 2022). The Pennine High was likely small in extent and/or elevation, implied by the lack of fluvial activity on the East Midlands Shelf (Howard et al., 2009; Jones et al., 2025).

Sediment routing over the London-Brabant and Welsh massifs remains poorly known owing to the absence of geological and mineralogical constraints in the Midlands and Worcester Graben. By area, these massifs are the second and third largest uplands after the Gallic Massif (**fig. 11**). Regionally, precipitation was highest in the south of the fairway, driven by Tethyan monsoons passing over the Variscan mountains (Péron et al., 2005; McKie, 2014; 2017). Lastly, the erodibility of the Palaeozoic sediments which cover the London-Brabant and Welsh massifs may be several times greater than the metamorphic-granitic basement of the Gallic Massif (Syvitski and Milliman, 2007). These lines of evidence suggest that comparatively large sediment fluxes from these uplands may have entered the Sherwood-2 River System in the Worcester Graben or Midlands basins. This sediment was likely lithic-rich and felspar-poor, containing lithoclasts of metasediments, volcanic rocks, carbonates and chert, and reflecting the mineralogy of recycled Devonian and Carboniferous sandstones (Knox et al., 1984; Glover and Powell, 1995; Bridge et al., 1998; Jones et al., 2011). Although bulk sandstone mineralogy clearly changes between the Wessex Basin and the Midlands, lithic fragments of the aforementioned nature are not reported from the northern part of the fairway. Here, lithics are composed of quartz and feldspar by the Gazzi-Dickinson method, which classifies lithic fragments by their constituent mineral phases (**fig. 8b**). Hence, changes in bulk mineralogy **(fig. 8b)** may not only be a product of interactions between different source areas, but may also result from the breakdown of recycled lithic fragments and feldspar during sediment transport and diagenesis. However, the ability of these processes to alter sandstone mineralogy has been questioned (Frings, 2008; Garzanti, 2019), and requires quantitative investigation.

Discussion and Conclusions

Overall, the stratigraphic architecture of Interval S2 is controlled by an increase in aridity and a series of frequent, but brief marine transgressions during the latter part of the Anisian (e.g. Newell, 2017a; McKie, 2017). The Sherwood-2 River System was initially externally draining, but continued aridification meant that for the majority of Interval S2, the fluvial system largely ended in terminal splay systems, discharging into a network of playa lakes with intermittent marine influence. Semiarid fluvial and aeolian deposits of the HSF were gradually replaced by mudstone-dominated playa and halite lake facies of the MMG (**fig. 4, 10a, b**).

Within Interval S2, the EISB is the largest sediment sink within the mapped fairway, representing 62% of the total sediment volume deposited during this interval (**fig. 7**). Although sand-grade sedimentation ceased during the deposition of the MMG, sediment fluxes were sufficient to fill basins. As previously discussed, calculated sediment accumulation rates were temporally variable, and likely controlled by differential tectonic subsidence (Newell, 2017a), although a paucity of chronostratigraphic constraints within Interval S2 limits the spatio-temporal resolution of this control.

North-flowing palaeocurrents in the HSF (**fig. 10a**) and the widespread distribution of Variscan-Cadomian material throughout the sediment fairway (e.g. Mange et al., 1999; Plant et al., 1999; Tyrrell et al., 2012; Morton et al., 2016), suggest that the Sherwood-2 River System was one, continuous river network. On the other hand, substantial changes in bulk sandstone mineralogy (**fig. 8b**) and differences in heavy mineral indices between basins (Plant et al., 1999; Morton et al., 2013) suggest sediment composition changes within the fairway. The HSF in the Wessex Basin is dominated by feldspathic sediments supplied from the Gallic Massif, which by area and elevation was the largest catchment feeding the Sherwood-2 River System (**fig. 11**). The bulk mineralogy of the HSF in the Wessex Basin contrasts with that of the Midlands basins, Cheshire Basin and EISB, where sediments are substantially more

quartz-rich (**fig. 8b**). This implies sediment composition was substantially modified in the Worcester Graben or the Midlands basins (**fig. 8a**), likely through substantial tributary input. In the Cheshire Basin and the EISB, fluvial and aeolian inputs of sediment are well-documented, and these basins were domains for considerable fluvial-aeolian interactions. Aeolian processes may have continued to be a substantial conveyor of sediment during the deposition of the MMG, and served to both import and export sediment from the fairway.

Evidence for additional fluvial inputs into the Sherwood-2 can be further observed when the fluvial systems of the SSG are compared to modern analogues in the Kati Thanda–Lake Eyre Basin (Brookfield, 2008; McKie 2014; Morón et al., 2014; English et al. 2024). Under semiarid climates and with no secondary inputs, these modern river systems experience high water transmission losses of around 80% over approximately 200 km (Costelloe et al., 2000), and are mostly ephemeral. Despite a comparable climatic setting, the Sherwood-2 River System was perennial in both its proximal and distal reaches over a length scale of 500km (Meadows and Beach, 1993; McKie et al., 1997; Meadows, 2006). As such, secondary fluvial inputs may have been important in maintaining a consistently perennial fluvial system, consistent with the substantial sediment inputs into the Sherwood-2 north of the Wessex Basin expressed in bulk sandstone mineralogy. Similarly, the decline of these proximal sources of sand during the onset of aridification may have contributed in generating the SSG-MMG transition, which occurred in the northern part of the fairway despite a sustained semiarid climate in the Wessex Basin (Newell, 2017b) and steady supply of fluvial sediment from the Gallic Massif recorded by the time-equivalent HSF there (Morton et al., 2016).

In conclusion, through the creation of a new chrono- and lithostratigraphic framework, and an updated paleogeographic framework for the mid-Triassic of the British Isles, we are able to resolve the spatial and temporal dynamics of the HSF, TSF and lower SMF, and construct a source-to-sink depositional model linking the three units. Our new synthesis of bulk sandstone mineralogy, supported by a synthesis of sediment routing and source area lithology shows that although the Sherwood-2 River System was a single fluvial system,

mineralogical changes occur between the south and north parts of the sediment fairway, suggesting that there were likely multiple, substantial sediment inputs north of the Wessex Basin. These tributaries likely drained from the London-Brabant and Welsh Massifs into the Midlands basins and Worcester Graben. The temporal evolution of the Sherwood-2 river system was dominated by a southwards retreat of fluvial deposits of the HSF, which were replaced by playa-lacustrine deposition of the TSF and SMF. This change is typically attributed to a regional increase in aridity. However, our results show a greater than fourfold increase in sediment accumulation rate in the EISB, the largest depocentre in the sediment fairway. As such, differential tectonic subsidence was likely a previously unrecognised control on stratigraphic architecture during this time interval.

Acknowledgements

We thank the UK Onshore Geophysical Library, the British Geological Survey, the Bureau de Recherches Géologiques et Minières, EDINA, and the North Sea Transition Authority National Data Repository for providing data used for analysis and visualisation in this study. We thank Neil Meadows and Stuart Burley for insightful discussions about the Sherwood Sandstone Group, and for supplying petrographic data. We thank Peter Burgess and an anonymous reviewer for their comments, which helped improve this paper.

Author contributions

XY: Conceptualization (lead), Data curation (lead), Formal analysis (lead), Investigation (lead), Methodology (lead), Visualization (lead), Writing – original draft (lead), Writing – review and editing (equal); **GJH:** Funding acquisition (lead), Methodology (supporting), Supervision (equal), Visualization (supporting), Writing – review and editing (equal); **ACW:** Funding

acquisition (supporting), Methodology (supporting), Supervision (equal), Visualization (supporting), Writing – review and editing (equal).

Funding

This work was funded by the Natural Environment Research Council (Grant NE/S007415/1).

Competing interests

The authors declare that they have no known competing financial interests or personal relationships that could have appeared to influence the work reported in this paper.

Data availability

All data generated or analysed during this study are included in this published article (and its supplementary material files).

References

Ainsworth, N.R. and Riley, L.A., 2010. Triassic to Middle Jurassic stratigraphy of the Kerr McGee 97/12-1 exploration well, offshore southern England. *Marine and Petroleum Geology*, *27*(4), pp.853-884. https://doi.org/10.1016/j.marpetgeo.2009.12.014

Ali, A.D., 1982. *Triassic stratigraphy and sedimentology in central England* (Doctoral dissertation, Aston University).

AlNajdi, N. and Worden, R.H., 2023. Porosity in mudstones and its effectiveness for sealing carbon capture and storage sites. *Geological Society, London, Special Publications*, *528*(1), pp.339-357. https://doi.org/10.1144/SP528-2022-84

Ambrose, K., Hough, E., Smith, N. J. P., and Warrington, G., 2014. Lithostratigraphy of the Sherwood Sandstone Group of England, Wales and south-west Scotland. British Geological Survey Research Report, RR/14/01.

Armitage, P.J., Worden, R.H., Faulkner, D.R., Aplin, A.C., Butcher, A.R. and Espie, A.A., 2013. Mercia Mudstone Formation caprock to carbon capture and storage sites: petrology and petrophysical characteristics. *Journal of the Geological Society*, *170*(1), pp.119-132. https://doi.org/10.1144/jgs2012-049

Arthurton, R.S., 1980. Rhythmic sedimentary sequences in the Triassic Keuper Marl (mercia mudstone group) of Cheshire, northwest England. *Geological Journal*, *15*(1), pp.43-58. https://doi.org/10.1002/gj.3350150106

Audley-Charles, M.G., 1970. Triassic palaeogeography of the British Isles. *Quarterly Journal of the Geological Society*, *126*(1-4), pp.49-74. https://doi.org/10.1144/gsjgs.126.1.0049

Augustsson, C., Voigt, T., Bernhart, K., Kreißler, M., Gaupp, R., Gärtner, A., Hofmann, M. and Linnemann, U., 2018. Zircon size-age sorting and source-area effect: The German Triassic Buntsandstein Group. *Sedimentary Geology*, *375*, pp.218-231. https://doi.org/10.1016/j.sedgeo.2017.11.004

Augustsson, C., 2021. Influencing factors on petrography interpretations in provenance research—a case-study review. *Geosciences*, *11*(5), p.205. https://doi.org/10.3390/geosciences11050205

Baptiste, J., 2016. *Cartographie structurale et lithologique du substratum du Bassin parisien et sa place dans la chaîne varisque de l'Europe de l'Ouest: approches combinées géophysiques, pétrophysiques, géochronologiques et modélisations 2D* (Doctoral dissertation, Université d'Orléans).

Barclay, W J, Ambrose, K, Chadwick, R A, and Pharaoh T C. 1997. Geology of the country around Worcester. Memoir of the British Geological Survey, Sheet 199 (England and Wales).

Bourquin, S., Bercovici, A., López-Gómez, J., Diez, J.B., Broutin, J., Ronchi, A., Durand, M., Arché, A., Linol, B. and Amour, F., 2011. The Permian–Triassic transition and the onset of Mesozoic sedimentation at the northwestern peri-Tethyan domain scale: palaeogeographic maps and geodynamic implications. *Palaeogeography, Palaeoclimatology, Palaeoecology*, *299*(1-2), pp.265-280. https://doi.org/10.1016/j.palaeo.2010.11.007

Bowman, M.B.J., McClure, N.M. and Wilkinson, D.W., 1993. Wytch Farm oilfield: deterministic reservoir description of the Triassic Sherwood Sandstone. In *Geological Society, London, Petroleum Geology Conference Series* (Vol. 4, No. 1, pp. 1513-1517). The Geological Society of London. https://doi.org/10.1144/0041513

Bray, R.J., Duddy, I.R. and Green, P.F., 1998. Multiple heating episodes in the Wessex Basin: implications for geological evolution and hydrocarbon generation. *Geological Society, London, Special Publications*, *133*(1), pp.199-213. https://doi.org/10.1144/GSL.SP.1998.133.01.09

Bridge, D McC, Carney, J N, Lawley, R S, and Rushton, A W A. 1998. Geology of the country around Coventry and Nuneaton. Memoir of the British Geological Survey, sheet 169 (England and Wales).

Bridge, D McC, and Hough, E. 2002. Geology of the Wolverhampton and Telford district. *Sheet description of the British Geological Survey,* 1:50 000 Series Sheet 153 (England and Wales).

Brookfield, M.E., 2008. Palaeoenvironments and palaeotectonics of the arid to hyperarid intracontinental latest Permian-late Triassic Solway basin (UK). *Sedimentary Geology*, *210*(1-2), pp.27-47. https://doi.org/10.1016/j.sedgeo.2008.06.003

Buchanan, J.G., 1998. The exploration history and controls on hydrocarbon prospectivity in the Wessex basins, southern England, UK. *Geological Society, London, Special Publications*, *133*(1), pp.19-37. https://doi.org/10.1144/GSL.SP.1998.133.01.02

Burgess, P.M., Dobromylskyj, E. and Lovell–Kennedy, J., 2025. Probably proximal pebbles? An outcrop-constrained quantitative analysis of clast transport distances in the lower Triassic Sherwood Sandstone Group, UK. *Journal of the Geological Society*, *182*(3), pp.jgs2024-155. https://doi.org/10.1144/jgs2024-155

Burley, S.D., 1984. Patterns of diagenesis in the Sherwood sandstone group (Triassic), United Kingdom. *Clay Minerals*, *19*(3), pp.403-440. https://doi.org/10.1180/claymin.1984.019.3.11

Burley, S.D., 1987. *Diagenetic modelling in the Triassic Sherwood sandstone group of England and its offshore equivalents, United Kingdom continental shelf* (Doctoral dissertation, University of Hull).

Busby, J.P. and Smith, N.J.P., 2001. The nature of the Variscan basement in southeast England: evidence from integrated potential field modelling. *Geological Magazine*, *138*(6), pp.669-685. https://doi.org/10.1017/S0016756801005751

Bushell, T.P., 1986. Reservoir geology of the Morecambe Field. *Geological Society, London, Special Publications*, *23*(1), pp.189-208. https://doi.org/10.1144/GSL.SP.1986.023.01.12

Butler, M., 1998. The geological history of the southern Wessex Basin—a review of new information from oil exploration. *Geological Society, London, Special Publications*, *133*(1), pp.67-86. https://doi.org/10.1144/GSL.SP.1998.133.01.04

Butler, M. 2019, Seismostratigraphic analysis of Palaeozoic sequences of the Midlands Microcraton. *Geological Society, London, Special Publications* 471, no. 1: 317-332. https://doi.org/10.1144/SP471.6

Carter, A., Yelland, A., Bristow, C. and Hurford, A.J., 1995. Thermal histories of Permian and Triassic basins in Britain derived from fission track analysis. *Geological Society, London, Special Publications*, *91*(1), pp.41-56. https://doi.org/10.1144/GSL.SP.1995.091.01.03

Castelltort, S., Fillon, C., Lasseur, É, Ortiz, A., Robin, C., Guillocheau, F., Tremblin, M., Bessin, P., Guerit, L., Dekoninck, A., Allanic, C., Gautheron, C., Barbarand, J., Loget, N., Uzel, J., Yans, J., Briais, J., Al-Reda, M., Baby, G., François, T., Roig, J. and Calassou, S. (2023). The Source-to-Sink Vade-mecum: History, Concepts and Tools. Society for Sedimentary Geology. CSP 16. https://doi.org/10.2110/sepmcsp.16

Chadwick, R.A. and Evans, D.J., 1995. The timing and direction of Permo-Triassic extension in southern Britain. *Geological Society, London, Special Publications*, *91*(1), pp.161-192. https://doi.org/10.1144/GSL.SP.1995.091.01.09

Chadwick, R. A., Jackson, D. I., Barnes, Kimbell, G. S., Johnson, H., Chiverrell, R. C., Thomas, G. S. P., Jones, N. S., Riley N. J., Pickett, E. A., Young, B., Holliday, D. W., Ball, D. F., Molyneux, S., Long, D., Power, G. M., and Roberts, D., 2001. Geology of the Isle of Man and its offshore area. (Keyworth, Nottingham: British Geological Survey and Treasury Isle of Man.)

Charsley, T. J., 1982. A standard nomenclature for the Triassic formations of the Ashbourne district. Report of the Institute of Geological Sciences, 81/14

Chedburn, L., Underhill, J.R., Head, S. and Jamieson, R., 2022. The critical evaluation of carbon dioxide subsurface storage sites: Geological challenges in the depleted fields of Liverpool Bay. *AAPG bulletin*, *106*(9), pp.1753-1789. https://doi.org/10.1306/07062221120

Chisholm, J. I., Charsley, T. J. And Aitkenhead, N. 1988. Geology of the country around Ashbourne and Cheadle. *Memoir of the British Geological Survey,* Sheet 124.

Cosgrove, G.I., Alkathery, M., Al-Masrahy, M., Colombera, L., Mountney, N.P. and Thompson, D.B., 2025. Quantitative sedimentological analysis of the aeolian–fluvial Triassic Sherwood Sandstone Group, Cheshire Basin, UK. *Sedimentology*, *72*(4), pp.1233-1274. https://doi.org/10.1111/sed.70000

Costelloe, J.F., Grayson, R.B. and McMahon, T.A., 2006. Modelling streamflow in a large anastomosing river of the arid zone, Diamantina River, Australia. *Journal of Hydrology*, *323*(1-4), pp.138-153. https://doi.org/10.1016/j.jhydrol.2005.08.022

Cowan, G., 1993. Identification and significance of aeolian deposits within the dominantly fluvial Sherwood Sandstone Group of the East Irish Sea Basin UK. *Geological Society, London, Special Publications*, *73*(1), pp.231-245. https://doi.org/10.1144/GSL.SP.1993.073.01.14

Croker, P. and Shannon, P. 1987. The evolution and hydrocarbon prospectivity of the Porcupine Basin, offshore Ireland. Conference on Petroleum Geology of North West Europe. Barbican Centre, London, 26-29 October, 3, pp.633–642.

De Sainz Simpson, R., 2022. *Sherwood Sandstone Outcrop Analogues Study in the Cheshire Basin: How to Better Constrain CCS Potential and Co2 Injectability in Depleted Oil and Gas Fields in the Context of the Liverpool Bay Carbon Capture Project* (Master's thesis, The University of Manchester (United Kingdom)).

Dercourt, J., Gaetani, M., Vrielynck, B., Barrier, E., Biju-Duval, B., Brunet, M.F., Cadet, J.P., Crasquin, S., Sandulescu, M., 2000. Atlas Peri-Tethys - Palaeogeographical maps. CCGM / CGMW Paris.

DiGRock250k [SHAPE geospatial data], Scale 1:250000, Tiles: GB, Updated: 31 December 2013, BGS, Using: EDINA Geology Digimap Service, <https://digimap.edina.ac.uk>, Downloaded: 2024-07-17 23:35:57.305

DiGRock625k [SHAPE geospatial data], Scale 1:625000, Tiles: GB, Updated: 31 December 2008, BGS, Using: Ordinance Survey, <https://osdatahub.os.uk/ >, Downloaded: 2023-11-23 13:34:58.

Donato, J.A., Pullan, C.P. and Dimitropoulos, K., 2023. Moho topography beneath England, the regional gravity field and speculations on crustal structure. UK Onshore Geophysical Library

Downing, R.A., Allen, D.J., Barker, J.A., Burgess, W.G., Gray, D.A., Price, M. and Smith, I.F., 1984. Geothermal exploration at Southampton in the UK: a case study of a low enthalpy resource. *Energy exploration and exploitation*, *2*(4), pp.327-342. https://doi.org/10.1177/014459878400200404

Dunford, G.M., Dancer, P.N. and Long, K.D., 2001. Hydrocarbon potential of the Kish Bank Basin: integration within a regional model for the Greater Irish Sea Basin. *Geological Society, London, Special Publications*, *188*(1), pp.135-154. https://doi.org/10.1144/GSL.SP.2001.188.01.07

Earp, J. R. and Taylor, B. J. 1986. Geology of the country around Chester and Winsford. Memoir British Geological Survey, Sheet 109 (England and Wales).

English, K.L., English, J.M., Moscardini, R., Haughton, P.D., Raine, R.J. and Cooper, M., 2024. Review of Triassic Sherwood Sandstone Group reservoirs of Ireland and Great Britain and their future role in geoenergy applications. *Geoenergy*, *2*(1), pp.geoenergy2023-042. https://doi.org/10.1144/geoenergy2023-042

Evans, D.J. and Holloway, S., 2009. A review of onshore UK salt deposits and their potential for underground gas storage. Geological Society, London, Special Publications, 313(1), pp.39-80. https://doi.org/10.1144/SP313.5

Evans, D.J., Rees, J.G. and Holloway, S., 1993. The Permian to Jurassic stratigraphy and structural evolution of the central Cheshire Basin. *Journal of the Geological Society*, *150*(5), pp.857-870. https://doi.org/10.1144/gsjgs.150.5.0857

Evans, D.J., Williams, J.D.O., Hough, E. and Stacey, A., 2011. The stratigraphy and lateral correlations of the Northwich and Preesall halites from the Cheshire Basin-East Irish Sea areas: implications for sedimentary environments, rates of deposition and the solution mining of gas storage caverns. In: SMRI Fall 2011 Technical Conference, York, UK, 2-4 Oct 2011.

Floodpage, J., Newman, P., White, J., 2001. Hydrocarbon prospectivity in the Irish Sea area: Insights from recent exploration of the Central Irish Sea, Peel and Solway basins. In: The Petroleum Exploration of Ireland's Offshore Basins, P. M. Shannon, P. D. W. Haughton, D. V. Corcoran (eds). The Petroleum Exploration of Ireland's Offshore Basins. Geological Society, London, Special Publications, 188, 107-134. https://doi.org/10.1144/GSL.SP.2001.188.01.06

Franklin, J., Tyrrell, S., O'Sullivan, G., Nauton-Fourteu, M. and Raine, R., 2020. Provenance of Triassic sandstones in the basins of Northern Ireland—Implications for NW European Triassic palaeodrainage. *Geological Journal*, *55*(7), pp.5432-5450. https://doi.org/10.1002/gj.3697

Frings, R.M., 2008. Downstream fining in large sand-bed rivers. *Earth-Science Reviews*, *87*(1-2), pp.39-60. http://doi.org/10.1016/j.earscirev.2007.10.001

Garzanti, E., 2017. The Maturity Myth In Sedimentology and Provenance Analysis. *Journal of Sedimentary Research* 2017;; 87 (4): 353–365. https://doi.org/10.2110/jsr.2017.17

Garzanti, E., 2019. Petrographic classification of sand and sandstone. *Earth-science reviews*, *192*, pp.545-563. https://doi.org/10.1016/j.earscirev.2018.12.014

Gent, C.M.A., 2016. Maturity modelling of well 110/07b- 6. British Geological Survey Commissioned Report, CR/16/043. 25pp.

Gibson-Poole, C.M., Tarasewicz, J., Gray, E., Hitchen, K., Bouffin, N., Taplin, M., Gillespie, A. and Buchanan, S.K., 2026. Endurance saline aquifer CO2 store–from appraisal to development and beyond. In: *Geological Society, London, Energy Geoscience Conference Series* (Vol. 1, No. 1, pp. egc1-2024). The Geological Society of London. https://doi.org/10.1144/egc1-2024-23

Glover, B.W. and Powell, J.H., 1996. Interaction of climate and tectonics upon alluvial architecture: Late Carboniferous-Early Permian sequences at the southern margin of the Pennine Basin, UK. *Palaeogeography, Palaeoclimatology, Palaeoecology*, *121*(1-2), pp.13-34. https://doi.org/10.1016/0031-0182(95)00050-X

Green, P.F., Thomson, K. and Hudson, J.D., 2001. Recognition of tectonic events in undeformed regions: contrasting results from the Midland Platform and East Midlands Shelf, Central England. *Journal of the Geological Society*, *158*(1), pp.59-73. https://doi.org/10.1144/jgs.158.1.59

Hallsworth, C.R., Morton, A.C., Claoué-Long, J. and Fanning, C.M., 2000. Carboniferous sand provenance in the Pennine Basin, UK: constraints from heavy mineral and detrital zircon age data. *Sedimentary Geology*, *137*(3-4), pp.147-185. https://doi.org/10.1016/S0037-0738(00)00153-6

Hamblin, R J O, Crosby, A, Balson, P S, Jones, S M, Chadwick, R A, Penn, I E, And Arthur, M J. 1992. United Kingdom offshore regional report. The geology of the English Channel, London: HMSO for the British Geological Survey

Hampson, G. J., Duller, R. A., Petter, A. L., Robinson, R. A. J. and Allen, P. A. (2014) Mass-Balance Constraints On Stratigraphic Interpretation of Linked Alluvial–Coastal–Shelf Deposits From Source To Sink: Example From Cretaceous Western Interior Basin, Utah and Colorado, U.S.A. Journal of Sedimentary Research. 84 (11), 935–960. https://doi.org/10.2110/jsr.2014.78

Hawkes, P.W., Fraser, A.J. and Einchcomb, C.C.G., 1998. The tectono-stratigraphic development and exploration history of the Weald and Wessex basins, Southern England, UK. *Geological Society, London, Special Publications*, *133*(1), pp.39-65. https://doi.org/10.1144/GSL.SP.1998.133.01.03

Head, S., Underhill, J.R., Jamieson, R. and Busch, A., 2026, April. Evaluating the role of cap rock in controlling natural accumulation and storage of carbon dioxide in the East Irish Sea Basin, UK. In *Geological Society, London, Energy Geoscience Conference Series* (Vol. 1, No. 1, pp. egc1-2024). The Geological Society of London. https://doi.org/10.1144/egc1-2024-10

Helland-Hansen, W., Sømme, T. O., Martinsen, O. J., Lunt, I. and Thurmond, J. (2016) Deciphering Earth's natural hourglasses; perspectives on source-to-sink analysis. Journal of Sedimentary Research. 86 (9), 1008-1033. https://doi.org/10.2110/jsr.2016.56

Herries, R.D. and Cowan, G., 1997. Challenging the 'sheetflood'myth: the role of water-table-controlled sabkha deposits in redefining the depositional model for the Ormskirk Sandstone Formation (Lower Triassic), East Irish Sea Basin. *Geological Society, London, Special Publications*, *124*(1), pp.253-276. https://doi.org/10.1144/GSL.SP.1997.124.01.16

Holliday, D.W., Williams, G.M., Holloway S., Savage D. and Bannon M.P, 1991. A Preliminary Feasibility Study for the Underground Disposal of Carbon Dioxide in UK. Nottingham, UK, British Geological Survey, 32pp. (WE/91/020) (Unpublished)

Hounslow, M.W. and McIntosh, G., 2003. Magnetostratigraphy of the Sherwood Sandstone Group (Lower and Middle Triassic), south Devon, UK: detailed correlation of the marine and non-marine Anisian. *Palaeogeography, Palaeoclimatology, Palaeoecology*, *193*(2), pp.325-348. https://doi.org/10.1016/S0031-0182(03)00235-9

Hounslow, M.W., McIntosh, G., Edwards, R.A., Laming, D.J. and Karloukovski, V., 2017. End of the Kiaman Superchron in the Permian of SW England: magnetostratigraphy of the Aylesbeare Mudstone and Exeter groups. *Journal of the Geological Society*, *174*(1), pp.56-74. https://doi.org/10.1144/jgs2015-141

Hounslow, M.W. and Gallois, R., 2023. Magnetostratigraphy of the Mercia Mudstone Group (Devon, UK): implications for regional relationships and chronostratigraphy in the Middle to Late Triassic of Western Europe. *Journal of the Geological Society*, *180*(4), pp.jgB2022-173. https://doi.org/10.1144/jgs2022-173

Howard, A S, Warrington, G, Ambrose, K, and Rees, J G. 2008. A formational framework for the Mercia Mudstone Group (Triassic) of England and Wales. British Geological Survey Research Report, RR/08/04.

Howard, A., Warrington, G., Carney, J., Ambrose, K., Young, S.R., Pharaoh, T. and Cheney, C., 2009. *Geology of the Nottingham district: memoir for 1: 50 000 geological sheet 126 (England and Wales)*. British Geological Survey.

1308 Ireland, R.J., Pollard, J.E., Steel, R.J. and Thompson, D.B., 1978. Intertidal sediments and trace
1309 fossils from the Waterstones (Scythian–Anisian?) at Daresbury, Cheshire. *Proceedings of the*
1310 *Yorkshire Geological Society*, *41*(4), pp.399-436. https://doi.org/10.1144/pygs.41.4.399

1311 Jackson, D. I., Jackson, A. A., Evans, D., Wingfield, R. T. R., Barnes, R. P., and Arthur, M. J., 1995.
1312 United Kingdom offshore regional report: the geology of the Irish Sea. (London: HMSO for the
1313 British Geological Survey.)

1314 Jackson, D.I., Johnson, H. and Smith, N.J.P., 1997. Stratigraphical relationships and a revised
1315 lithostratigraphical nomenclature for the Carboniferous, Permian and Triassic rocks of the
1316 offshore East Irish Sea Basin. *Geological Society, London, Special Publications*, *124*(1), pp.11-
1317 32. https://doi.org/10.1144/GSL.SP.1997.124.01.02

1318 Jeans, C.V., 2006. Clay mineralogy of the Permo-Triassic strata of the British Isles: onshore and
1319 offshore. *Clay Minerals*, *41*(1), pp.309-354. https://doi.org/10.1180/0009855064110199

1320 Jefferson, I., Rosenbaum, M. and Smalley, I., 2002. Mercia Mudstone as a Triassic aeolian desert
1321 sediment. *Mercian Geologist*, *15*(3), pp.157-162.

1322 Jones, N.S. and Ambrose, K., 1994. Triassic sandy braidplain and aeolian sedimentation in the
1323 Sherwood Sandstone Group of the Sellafield area, west Cumbria. *Proceedings of the Yorkshire*
1324 *Geological Society*, *50*(1), pp.61-76. https://doi.org/10.1144/pygs.50.1.61

1325 Jones, N.S., Holliday, D.W. and McKERVEY, J.A., 2011. Warwickshire Group (Pennsylvanian) red-
1326 beds of the Canonbie Coalfield, England–Scotland border, and their regional
1327 palaeogeographical implications. *Geological Magazine*, *148*(1), pp.50-77.
1328 https://doi.org/10.1017/S001675681000035X

1329 Jones, S.T., Worden, R.H., Faulkner, D.R., Fisher, Q.J., McEvoy, J.A. and Utley, J.E., 2025.
1330 Deposition, diagenesis, and porosity of a siliciclastic caprock: the Late Triassic Mercia
1331 Mudstone Group. *Journal of the Geological Society*, pp.jgs2025-086.
1332 https://doi.org/10.1144/jgs2025-086

1333 Knox, R.O.B., Burgess, W.G., Wilson, K.S. and Bath, A.H., 1984. Diagenetic influences on reservoir
1334 properties of the Sherwood Sandstone (Triassic) in the Marchwood geothermal borehole,

Southampton, UK. *Clay Minerals*, *19*(3), pp.441-456. https://doi.org/10.1180/claymin.1984.019.3.12

Lang, S.C., Payenberg, T.H.D., Reilly, M.R.W., Hicks, T., Benson, J. and Kassan, J., 2004. Modern analogues for dryland sandy fluvial-lacustrine deltas and terminal splay reservoirs. *The APPEA Journal*, *44*(1), pp.329-356. https://doi.org/10.1071/AJ03012

Mange, M., Turner, P., Ince, D., Pugh, J. and Wright, D., 1999. A new perspective on the zonation and correlation of barren strata: an integrated heavy mineral and palaeomagnetic study of the Sherwood Sandstone Group, East Irish Sea Basin and surrounding areas. *Journal of Petroleum Geology*, *22*(3), pp.325-348. https://doi.org/10.1111/j.1747-5457.1999.tb00990.x

Mange, M.A., Turner, P., Ince, D. and Wright, D.T., 2007. High-resolution heavy mineral-and magnetostratigraphy; a powerful tool for subdivision and correlation of barren successions: An example from the Sherwood Sandstone Group (Triassic) of the East Irish Sea Basin and surrounding areas. *Developments in Sedimentology*, *58*, pp.1073-1097. https://doi.org/10.1016/S0070-4571(07)58042-8

Mao, X., Liu, X. and Zhou, X., 2021. Permo-Triassic aeolian red clay of southwestern England and its palaeoenvironmental implications. *Aeolian Research*, *52*, p.100726. https://doi.org/10.1016/j.aeolia.2021.100726

Markwick, P. J. (2019) Palaeogeography in exploration. Geological Magazine. 156 (2), 366-407. https://doi.org/10.1017/S0016756818000468

Marsh, J.R., Jones, S.J., Meadows, N.S. and Gluyas, J.G., 2022. Petrographic and diagenetic investigation of the distal Triassic ‘Budleighensis’ fluvial system in the Solway and Carlisle Basins for potential CO2 storage. *Petroleum Geoscience*, *28*(3), pp.petgeo2021-065. https://doi.org/10.1144/petgeo2021-065

Martínez Catalán, J.R., Schulmann, K. and Ghienne, J.F., 2021. The Mid-Variscan Allochthon: Keys from correlation, partial retrodeformation and plate-tectonic reconstruction to unlock the geometry of a non-cylindrical belt. *Earth-Science Reviews*, *220*, p.103700. https://doi.org/10.1016/j.earscirev.2021.103700

Marx, S.K., May, J-H., Cohen. T., Kamber. B.S., McGowan, H.A. and Petherick L. (2022). Dust emissions from Kati Thanda-Lake Eyre: a review. Transactions of the Royal Society of South Australia, 146:1, 168-206, https://doi.org/10.1080/03721426.2022.2054918

McKie, T., Aggett, J. and Hogg, A.J.C., 1997. Sequence architecture of a Triassic semi-arid, fluvio-lacustrine reservoir, Wytch Farm Field, southern England. In: GCSSEPM Foundation 18th Annual Research Conference Shallow Marine and Nonmarine Reservoirs, December 7-10, 1997. https://doi.org/10.5724/gcs.97.18.0197

Mckie, T., 2011. A comparison of modern Dryland depositional systems with the Rotliegend group in the Netherlands. SEPM Special Publications. 98. 89-103. https://doi.org/10.2110/pec.11.98.0089.

Mckie, T., 2014. Climatic and tectonic controls on Triassic dryland terminal fluvial system architecture, central North Sea. In: Martinius, A.W., Ravnås, R., Howell, J.A., Steel, R.J. and Wonham, J.P. (eds) From Depositional Systems to Sedimentary Successions on the Norwegian Continental Shelf. Blackwell, Oxford, 46, 19–58 [IAS Special Publication]. https://doi.org/10.1002/9781118920435.ch2

McKie, T., 2017. Palaeogeographic evolution of latest Permian and Triassic salt basins in Northwest Europe. In: Soto, J. I., Flinch, J. F. and Tari, G. (eds.) *Permo-triassic salt provinces of Europe, North Africa and the Atlantic margins* (pp. 159-173). Elsevier. https://doi.org/10.1016/B978-0-12-809417-4.00008-2

Meadows, N.S., 2006. The correlation and sequence architecture of the Ormskirk sandstone formation in the Triassic Sherwood sandstone group of the East Irish Sea Basin, NW England. *Geological Journal*, *41*(1), pp.93-122. https://doi.org/10.1002/gj.1034

Meadows, N. S., Director at Redrock Associates Int Ltd (Personal communication, 3rd March 2025)

Meadows, N.S. and Beach, A., 1993a. Controls on reservoir quality in the Triassic Sherwood Sandstone of the Irish Sea. In *Geological Society, London, Petroleum Geology Conference Series* (Vol. 4, No. 1, pp. 823-833). The Geological Society of London. https://doi.org/10.1144/0040823

1389 Meadows, N.S. and Beach, A., 1993b. Structural and climatic controls on facies distribution in a mixed
1390 fluvial and aeolian reservoir: the Triassic Sherwood Sandstone in the Irish Sea. *Geological*
1391 *Society, London, Special Publications*, *73*(1), pp.247-264.
1392 https://doi.org/10.1144/GSL.SP.1993.073.01.15

1393 Medici, G., West, L.J. and Mountney, N.P., 2019a. Sedimentary flow heterogeneities in the Triassic
1394 UK Sherwood Sandstone Group: insights for hydrocarbon exploration. *Geological*
1395 *Journal*, *54*(3), pp.1361-1378. https://doi.org/10.1002/gj.3233

1396 Medici, G., West, L.J., Mountney, N.P. and Welch, M., 2019b. Permeability of rock discontinuities and
1397 faults in the Triassic Sherwood Sandstone Group (UK): insights for management of fluvio-
1398 aeolian aquifers worldwide. Hydrogeology Journal, 27(8), pp.2835-2855.
1399 https://doi.org/10.1007/s10040-019-02035-7

1400 Mikkelsen, P.W. and Floodpage, J.B., 1997. The hydrocarbon potential of the Cheshire
1401 Basin. *Geological Society, London, Special Publications*, *124*(1), pp.161-183.
1402 https://doi.org/10.1144/GSL.SP.1997.124.01.10

1403 Merlin Energy Resources Consortium, 2020. The Standard Stratigraphic Nomenclature of Offshore
1404 Ireland: An Integrated Lithostratigraphic, Biostratigraphic and Sequence Stratigraphic
1405 Framework. Project Atlas. Petroleum Affairs Division, Department of the Environment (DEEC),
1406 Climate and Communications, Special Publication, 1/21.

1407 Michael, N.A. and Zühlke, R., 2022. Source-to-sink: Regional grain size trends to reconstruct
1408 sediment budgets and catchment areas. *Basin Research*, *34*(1), pp.393-410.
1409 https://doi.org/10.1111/bre.12624

1410 Miliorizos, M. and Ruffell, A., 1998. Kinematics of the Watchet-Cothelstone-Hatch fault system:
1411 implications for the fault history of the Wessex basin and adjacent areas. Geological Society,
1412 London, Special Publications, 133(1), pp.311-330.
1413 https://doi.org/10.1144/GSL.SP.1998.133.01.15

1414 Morón, S., Amos, K. and Mann, S., 2014. Fluvial reservoirs in dryland endorheic basins: the Lake
1415 Eyre Basin as a world-class modern analogue. *The APPEA Journal*, *54*(1), pp.119-134.
1416 https://doi.org/10.1071/AJ13014

1417 Morton, A.C., Chisholm, J.I. and Frei, D., 2021. Provenance of Carboniferous sandstones in the
1418 central and southern parts of the Pennine Basin, UK: evidence from detrital zircon
1419 ages. *Proceedings of the Yorkshire Geological Society*, *63*(3), pp.pygs2020-010.
1420 https://doi.org/10.1144/pygs2020-010

1421 Morton, A.C., Chisholm, J.I. and Frei, D., 2024. Provenance response to evolving palaeogeography
1422 recorded by Carboniferous sandstones in the northern Pennine Basin, UK. *Sedimentary*
1423 *Geology*, *470*, p.106691. https://doi.org/10.1016/j.sedgeo.2024.106691

1424 Morton, A.C. and Hallsworth, C., 1994. Identifying provenance-specific features of detrital heavy
1425 mineral assemblages in sandstones. *Sedimentary Geology*, *90*(3-4), pp.241-256.
1426 https://doi.org/10.1016/0037-0738(94)90041-8

1427 Morton, A., Hounslow, M.W. and Frei, D., 2013. Heavy-mineral, mineral-chemical and zircon-age
1428 constraints on the provenance of Triassic sandstones from the Devon coast, southern
1429 Britain. *Geologos*, *19*(1-2), pp.67-85. https://doi.org/10.2478/logos-2013-0005

1430 Morton, A., Knox, R. and Frei, D., 2016. Heavy mineral and zircon age constraints on provenance of
1431 the Sherwood Sandstone Group (Triassic) in the eastern Wessex Basin, UK. *Proceedings of*
1432 *the Geologists' Association*, *127*(4), pp.514-526. https://doi.org/10.1016/j.pgeola.2016.06.001

1433 Mountney, N.P. and Thompson, D.B., 2002. Stratigraphic evolution and preservation of aeolian dune
1434 and damp/wet interdune strata: an example from the Triassic Helsby Sandstone Formation,
1435 Cheshire Basin, UK. *Sedimentology*, *49*(4), pp.805-833. https://doi.org/10.1046/j.1365-
1436 3091.2002.00472.x

1437 Naylor, D., Haughey, N., Clayton, G. and Graham, J.R., 1993. The Kish Bank Basin, offshore Ireland.
1438 In *Geological Society, London, Petroleum Geology Conference Series* (Vol. 4, No. 1, pp. 845-
1439 855). The Geological Society of London. https://doi.org/10.1144/0040845

1440 Newell, A. J., 2017a. Rifts, rivers and climate recovery: A new model for the Triassic of
1441 England. *Proceedings of the Geologists' Association*, *129*(3), pp.352-371.
1442 https://doi.org/10.1016/j.pgeola.2017.04.001

1443 Newell, A. J., 2017b. Evolving stratigraphy of a Middle Triassic fluvial-dominated sheet sandstone:
1444 The Otter Sandstone Formation of the Wessex Basin (UK). *Geological Journal*, *53*(5), pp.1954-
1445 1972. https://doi.org/10.1002/gj.3026

1446 Newell, A. J., 2023 *The Sherwood Sandstone and Bacton groups of the East Midlands Shelf – an*
1447 *onshore to offshore correlation using outcrop evidence and geophysical logs.* Nottingham, UK,
1448 British Geological Survey.

1449 Newell, A. 2024. UK Stratigraphical Framework Series: Mercia Mudstone Group. British Geological
1450 Survey Open Report, OR/24/046. 77pp.

1451 Newell, A.J. and Shariatipour, S.M., 2016. Linking outcrop analogue with flow simulation to reduce
1452 uncertainty in sub-surface carbon capture and storage: an example from the Sherwood
1453 Sandstone Group of the Wessex Basin, UK. *Geological Society, London, Special*
1454 *Publications*, *436*(1), pp.231-246. https://doi.org/10.1144/SP436

1455 Newell, A J, Smith, N J., 2009. Bromsgrove Aquifer Groundwater Modelling Study: Results from Task
1456 1.1 3D Visualisation and Geological Framework of the Bromsgrove Aquifer. British Geological
1457 Survey Commissioned Report, CR/09/023. 18pp.

1458 Newman, P.J., 1999. The geology and hydrocarbon potential of the Peel and Solway Basins, East
1459 Irish Sea. *Journal of Petroleum Geology*, *22*(3), pp.305-324. https://doi.org/10.1111/j.1747-
1460 5457.1999.tb00989.x

1461 Ogg, J. G., Chen, Z.-Q., Orchard, M. J., Jiang, H. S., 2020. Chapter 25 - The Triassic Period. In:
1462 Gradstein, F. M., Ogg, J. G., Schmitz, M. D., Ogg G. M., Geologic Time Scale, (pp. 903-953)
1463 Elsevier, https://doi.org/10.1016/B978-0-12-824360-2.00025-5.

1464 Old, R. A., Sumbler, M. G. and Ambrose, K. 1987. Geology of the country around Warwick. *Memoir of*
1465 *the British Geological Survey*, Sheet 184 (England and Wales).

1466 Old, R A, Hamblin, R J O, Ambrose, K, and Warrington, G. 1991. Geology of the country around
1467 Redditch. Memoir of the British Geological Survey, Sheet 183 (England and Wales).

1468 Paola, C., Martin, J. M., 2012. Mass-Balance Effects In Depositional Systems. *Journal of Sedimentary*
1469 *Research,* 82 (6), pp.435–450. https://doi.org/10.2110/jsr.2012.38

Parkes, D., Busby, J., Kemp, S.J., Petitclerc, E. and Mounteney, I., 2021. The thermal properties of the Mercia Mudstone Group. *Quarterly Journal of Engineering Geology and Hydrogeology*, *54*(2), pp.qjegh2020-098. https://doi.org/10.1144/qjegh2020-098

Paul, J., Wemmer, K. and Ahrendt, H., 2008. Provenance of siliciclastic sediments (Permian to Jurassic) in the Central European Basin. *Zeitschrift der Deutschen Gesellschaft fur Geowissenschaften*, *159*(4), pp.641-650. https://doi.org/10.1127/1860-1804/2008/0159-0641

Péron, S., Bourquin, S., Fluteau, F. and Guillocheau, F., 2005. Palaeoenvironment reconstructions and climate simulations of the Early Triassic: impact of the water and sediment supply on the preservation of fluvial systems. *Geodinamica Acta*, *18*(6), pp.431-446. https://doi.org/10.3166/ga.18.431-446

Pharaoh, T.C., Gent, C.M.A., Hannis, S.D., Kirk, K.L., Monaghan, A.A., Quinn, M.F., Smith, N.J.P., Vane, C.H., Wakefield, O. and Waters, C.N., 2019. An overlooked play? Structure, stratigraphy and hydrocarbon prospectivity of the Carboniferous in the East Irish Sea–North Channel basin complex. *Geological Society, London, Special Publications*, *471*(1), pp.281-316. https://doi.org/10.1144/SP471.7

Pharaoh, T., Jones, D., Kearsey, T., Newell, A., Abesser, C., Randles, T., Patton, A. and Kendall, R., 2021. Early Carboniferous limestones of southern and central Britain: Characterisation and preliminary assessment of deep geothermal prospectivity. Zeitschrift der Deutschen Gesellschaft für Geowissenschaften, 172(3), pp.227-249. https://doi.org/172. 10.1127/zdgg/2021/0282

Plant, J. A., Jones, D. G., and Haslam, H W (editors). 1999. The Cheshire Basin: Basin evolution, fluid movement and mineral resources in a Permo-Triassic rift setting. Keyworth, Nottingham: for the British Geological Survey.

Pullan, C. P., Donato, J. A., 2022. The Eastern Extension of Southwest England under the Mesozoic Southern England Basin and its Variscan Dextral Translation. UK Onshore Geophysical Library.

Radley, J.D. and Coram, R.A., 2016. The Chester Formation (Early Triassic, southern Britain): sedimentary response to extreme greenhouse climate?. *Proceedings of the Geologists' Association*, *127*(5), pp.552-557. https://doi.org/10.1016/j.pgeola.2016.08.002

Ravidà, D.C., Caracciolo, L., Heins, W.A. and Stollhofen, H., 2021. Reconstructing environmental signals across the Permian-Triassic boundary in the SE Germanic basin: Palaeodrainage modelling and quantification of sediment flux. *Global and Planetary Change*, *206*, p.103632. https://doi.org/10.1016/j.gloplacha.2021.103631

Rees, J G, and Wilson, A A. 1998. Geology of the country around Stoke-on-Trent. Memoir of the Geological Survey, Sheet 123 (England and Wales).

Reynolds, T., 2024. Grain size from source to sink–modern and ancient fining rates. *Earth-Science Reviews*, *250*, p.104699. https://doi.org/10.1016/j.earscirev.2024.104699

Rhys, G.H., 1982. The Winterborne Kingston borehole, Dorset, England. Report of the Institute of Geological Sciences, No. 81/3.

Romans, B. W. and Graham, S. A. (2013) A Deep-Time Perspective of Land-Ocean Linkages in the Sedimentary Record. Annual Review of Marine Science. 5, 69-94. https://doi.org/10.1146/annurev-marine-121211-172426

Ruffell, A., Coward, M.P. and Harvey, M., 1995. Geometry and tectonic evolution of megasequences in the Plymouth Bay Basin, English Channel. Geological Society, London, Special Publications, 91(1), pp.193-214. https://doi.org/10.1144/GSL.SP.1995.091.01.10

Sánchez Martínez, S., De la Horra, R., Arenas, R., Gerdes, A., Galán-Abellán, A.B., López-Gómez, J., Barrenechea, J.F. and Arche, A., 2012. U-Pb ages of detrital zircons from the Permo-Triassic series of the Iberian Ranges: a record of variable provenance during rift propagation. *The Journal of Geology*, *120*(2), pp.135-154. https://doi.org/10.1086/663983

Sass, K., von Eynatten, H., Meyerink, T., Schade, J. and Dunkl, I., 2023. Heavy mineral constraints on the evolution and provenance of upper Permian and lower Triassic siliciclastic deposits of the Central European Basin. *Journal of Applied and Regional Geology/Zeitschrift der Deutschen Gesellschaft für Geowissenschaften (ZDGG)*, *174*(3). https://doi.org/10.1127/zdgg/2023/0404

Scorgie, J.C., Worden, R.H., Utley, J.E.P. and Roche, I.P., 2021. Reservoir quality and diagenesis of Triassic sandstones and siltstones from arid fluvial and playa margin environments: a study of one of the UK's earliest producing oilfields. *Marine and Petroleum Geology*, *131*, p.105154. https://doi.org/10.1016/j.marpetgeo.2021.105154

Searle, M.P., Shail, R.K., Pownall, J.M., Jurkowski, C., Watts, A.B. and Robb, L.J., 2024. The Permian Cornubian granite batholith, SW England; Part 1: Field, structural, and petrological constraints. *Geological Society of America Bulletin*, *136*(9-10), pp.4301-4320. https://doi.org/10.1130/B37457.1

Shail, R.K. and Leveridge, B.E., 2009. The Rhenohercynian passive margin of SW England: Development, inversion and extensional reactivation. *Comptes Rendus. Géoscience*, *341*(2-3), pp.140-155. https://doi.org/10.1016/j.crte.2008.11.002

Simms, M., 2009. The Permian and Mesozoic. In: Holland, C. H., Sanders, I. (eds). The Geology of Ireland (pp. 331-332). Liverpool University Press. https://doi.org/10.2307/jj.12638997.16

Smith, S.A. and Edwards, R.A., 1991. Regional sedimentological variations in Lower Triassic fluvial conglomerates (Budleigh Salterton Pebble Beds), southwest England: some implications for palaeogeography and basin evolution. *Geological Journal*, *26*(1), pp.65-83. https://doi.org/10.1002/gj.3350260105

Sømme, T. O., Helland-Hansen, W., Martinsen, O. J., Thurmond, J.B. (2009) Relationships between morphological and sedimentological parameters in source-to-sink systems: a basis for predicting semi-quantitative characteristics in subsurface systems. Basin Research. 21, 361-387. https://doi.org/10.1111/j.1365-2117.2009.00397.x

Strong, G.E. and Milodowski, A.E., 1987. Aspects of the diagenesis of the Sherwood Sandstones of the Wessex Basin and their influence on reservoir characteristics. *Geological Society, London, Special Publications*, *36*(1), pp.325-337. https://doi.org/10.1144/GSL.SP.1987.036.01.23

Sumbler, M G, Barron, A J M, and Morigi, A N., 2000. Geology of the Cirencester district. Memoir of the British Geological Survey, Sheet 235 (England and Wales).

Sun, Y., Joachimski, M.M., Wignall, P.B., Yan, C., Chen, Y., Jiang, H., Wang, L. and Lai, X., 2012. Lethally hot temperatures during the Early Triassic greenhouse. *Science*, *338*(6105), pp.366-370. https://www.science.org/doi/10.1126/science.1224126

Svendsen, J.B. and Hartley, N.R., 2001. Comparison between outcrop-spectral gamma ray logging and whole rock geochemistry: implications for quantitative reservoir characterisation in

continental sequences. *Marine and Petroleum Geology*, *18*(6), pp.657-670. https://doi.org/10.1016/S0264-8172(01)00022-8

Syvitski, J.P. and Milliman, J.D., 2007. Geology, geography, and humans battle for dominance over the delivery of fluvial sediment to the coastal ocean. *The Journal of Geology*, *115*(1), pp.1-19.

Thomas, L.P.; Holliday, D.W., 1982 Southampton no.1 (Western Esplanade) geothermal well: geological well completion report. Institute of Geological Sciences, 41pp. (WA/KB/82/003) (Unpublished)

Thompson, D.B., 1970a. The stratigraphy of the so-called Keuper Sandstone Formation (Scythian–? Anisian) in the Permo–Triassic Cheshire Basin. *Quarterly Journal of the Geological Society*, *126*(1-4), pp.151-181. https://doi.org/10.1144/gsjgs.126.1.0151

Thompson, D.B., 1970b. Sedimentation of the Triassic (Scythian) red pebbly sandstones in the Cheshire Basin and its margins. *Geological Journal*, *7*(1), pp.183-216. https://doi.org/10.1002/gj.3350070111

Thompson, J. and Meadows, N.S., 1997. Clastic sabkhas and diachroneity at the top of the Sherwood Sandstone Group: East Irish Sea Basin. *Geological Society, London, Special Publications*, *124*(1), pp.237-251. https://doi.org/10.1144/GSL.SP.1997.124.01.15

Tyrrell, S., Haughton, P.D., Souders, A.K., Daly, J.S. and Shannon, P.M., 2012. Large-scale, linked drainage systems in the NW European Triassic: insights from the Pb isotopic composition of detrital K-feldspar. *Journal of the Geological Society*, *169*(3), pp.279-295. https://doi.org/10.1144/0016-76492011-104

Underhill, J. and Stoneley, R., 1998, Introduction to the development, evolution and petroleum geology of the Wessex Basin, Geological Society Special Publications, vol. 133, pp. 1-18. https://doi.org/10.1144/GSL.SP.1998.133.01.01

Walsh, P.T., Banks, V.J., Jones, P.F., Pound, M.J. and Riding, J.B., 2018. A reassessment of the Brassington Formation (Miocene) of Derbyshire, UK and a review of related hypogene karst suffosion processes. *Journal of the Geological Society*, *175*(3), pp.443-463. https://doi.org/10.1144/jgs2017-029

Walsh, P.T., Collins, P., Ijtaba, M., Newton, J.P., Scott, N.H. and Turner, P.R., 1980. Palaeocurrent directions and their bearing on the origin of the Brassington Formation (Miocene-Pliocene) of the southern Pennines, Derbyshire, England, Mercian Geologist, 8(1), pp.47-61

Warrington, G., 1970a. The “Keuper” Series of the British Trias in the northern Irish Sea and neighbouring areas. *Nature*, *226*(5242), pp.254-256. https://doi.org/10.1038/226254a0

Warrington, G., 1970b. The stratigraphy and palaeontology of the 'Keuper' Series of the central Midlands of England. *Quarterly Journal of the Geological Society*, *126*(1-4), pp.183-223. https://doi.org/10.1144/gsjgs.126.1.0183

Warrington, G. and Ivimey-Cook, H.C., 1992. Triassic. In: Cope, J.C.W., Ingham, J.K. and Rawson, P.F. (eds) Atlas of Palaeogeography and Lithofacies. Memoirs of the Geological Society of London, 13, 97-106. https://doi.org/10.1144/GSL.MEM.1992.013.01.11

Warrington, G. and Pollard, J.E., 2021. On the records of the brachiopod ‘Lingula’and associated fossils in Mid-Triassic deposits in England. *Proceedings of the Yorkshire Geological Society*, *63*(4), pp.pygs2020-015. https://doi.org/10.1144/pygs2020-015

Wills, L. J. (1956). Concealed coalfields: a palaeographical study of the stratigraphy and tectonics of mid-England in relation to coal reserves. London: Blackie.

Wills, L.J., 1970. The Triassic succession in the central Midlands in its regional setting. *Quarterly Journal of the Geological Society*, *126*(1-4), pp.225-283. https://doi.org/10.1144/gsjgs.126.1.0225

Wills, L. J. (1976). The Trias of Worcestershire and Warwickshire. Report (Institute of Geological Sciences (Great Britain)), 76/2. London : HMSO.

Wilson, A.A., 1990. The Mercia Mudstone Group (Trias) of the East Irish Sea Basin. *Proceedings of the Yorkshire Geological Society*, *48*(1), pp.1-22. https://doi.org/10.1144/pygs.48.1.1

Wilson, A. A., 1993. The Mercia Mudstone Group (Trias) of the Cheshire Basin. *Proceedings of the Yorkshire Geological Society*, *49*(3), pp.171-188. https://doi.org/10.1144/pygs.49.3.171

Wilson, A. A. and Evans, W. B. 1990. Geology of the country around Blackpool. *Memoir of the British Geological Survey,* Sheet 66 (England and Wales).

Wrobel-Daveau, J., Nicoll, G., Tetley, M. G., Gréselle, B., Perez-Diaz, L., Davies, A. and Eglington, B. M. (2022) Plate tectonic modelling and the energy transition. Earth-Science Reviews. 234, 104227. https://doi.org/10.1016/j.earscirev.2022.104227

Yu9824, 2021. Ternary Diagram. https://github.com/yu9824/ternary-diagram/. Accessed 28th November 2024

Table 1: List of commonly abbreviated stratigraphic and paleogeographic terms used in text.

Abbreviation	Full name
CHF	Chester Formation (Sherwood Sandstone Group)
EISB	East Irish Sea Basin
HSF	Helsby Sandstone Formation (Sherwood Sandstone Group)
MMG	Mercia Mudstone Group
MTU	Mid-Triassic Unconformity (former Hardegsen Unconformity)
SMF	Sidmouth Mudstone Formation (Mercia Mudstone Group)
SSG	Sherwood Sandstone Group
TSF	Tarporley Siltstone Formation (Mercia Mudstone Group)
WSF	Wilmslow Sandstone Formation (Sherwood Sandstone Group)

Table 2: Key sedimentological parameters for the Helsby Sandstone Formation (HSF) in each sedimentary basin in the mapped fairway (**fig. 3**). Median porosities compiled by Medici et al. (2019a), except the Wessex Basin (estimated from Bowman et al., 1993; Newell and Shariatipour, 2016). Estimated proportion of fluvial and aeolian deposits compiled from Thompson et al. (1970), Meadows and Beach (1994b), McKie et al. (1997), Ambrose et al. (2014), Newell (2018b).

Basin	Wessex	Worcester	Midlands	Cheshire	East Irish Sea
Median porosity (%)	18.0	14.8	26.9	24.0	12.7
Proportion of fluvial deposits (%)	90	100	100	71	64
Proportion of aeolian deposits (%)	10	0	0	29	36

Table 3: Summary statistics for petrographic data within the Helsby Sandstone Formation (HSF), grouped by study, by point count method (Augustsson et al., 2021), and by basin.

	Point count method	Wessex Basin (W)	Wessex Basin (E)	Worcester Graben	Midlands Basins	Cheshire Basin	East Irish Sea Basin
Meadows, pers comms.	Traditional					10	121
De Sainz Simpson, 2022	Gazzi-Dickinson					41	44
Scorgie et al., 2021	Traditional						12
Svendsen and Hartley, 2001	Gazzi-Dickinson	23					
Chisholm et al., 1988	Unclassified				1		
Burley, 1987	Traditional	9	11			11	18
Knox et al., 1984	Gazzi – Dickinson		14				
Ali et al., 1982	Unclassified				5		

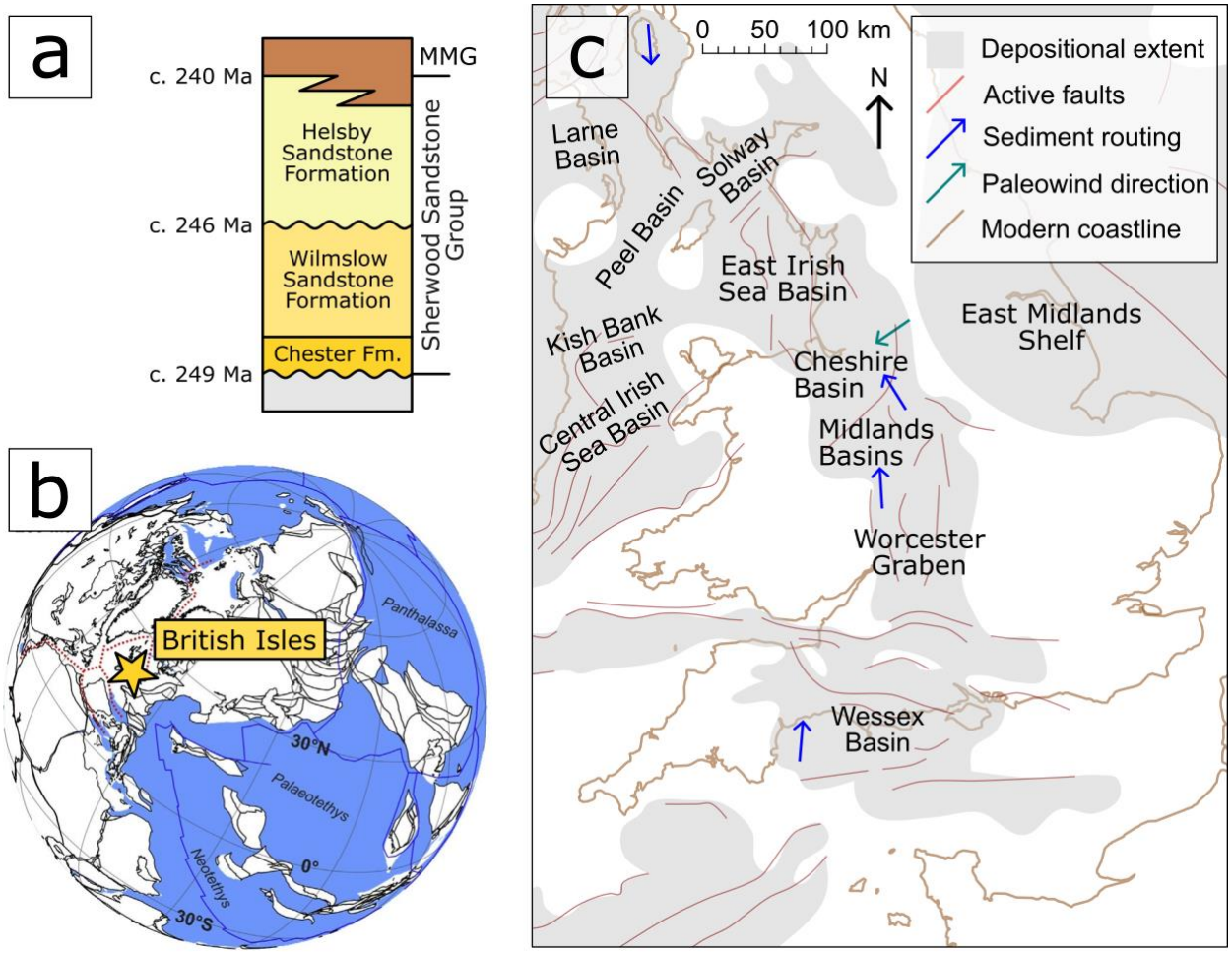

1623

1624 **Figure 1: (a)** General stratigraphy (Ambrose et al., 2023) and ages (Hounslow and
1625 McIntosh, 2003; Hounslow and Gallois, 2023) of the lower and middle Triassic
1626 succession of the British Isles, comprising the Sherwood Sandstone Group and Mercia
1627 Mudstone Group (MMG). **(b)** Global position of the British Isles during the lower Triassic,
1628 adapted from Newell (2017a). **(c)** General basin configuration of the British Isles during
1629 the mid-Triassic. Adapted from Warrington and Ivimey-Cook (1992).

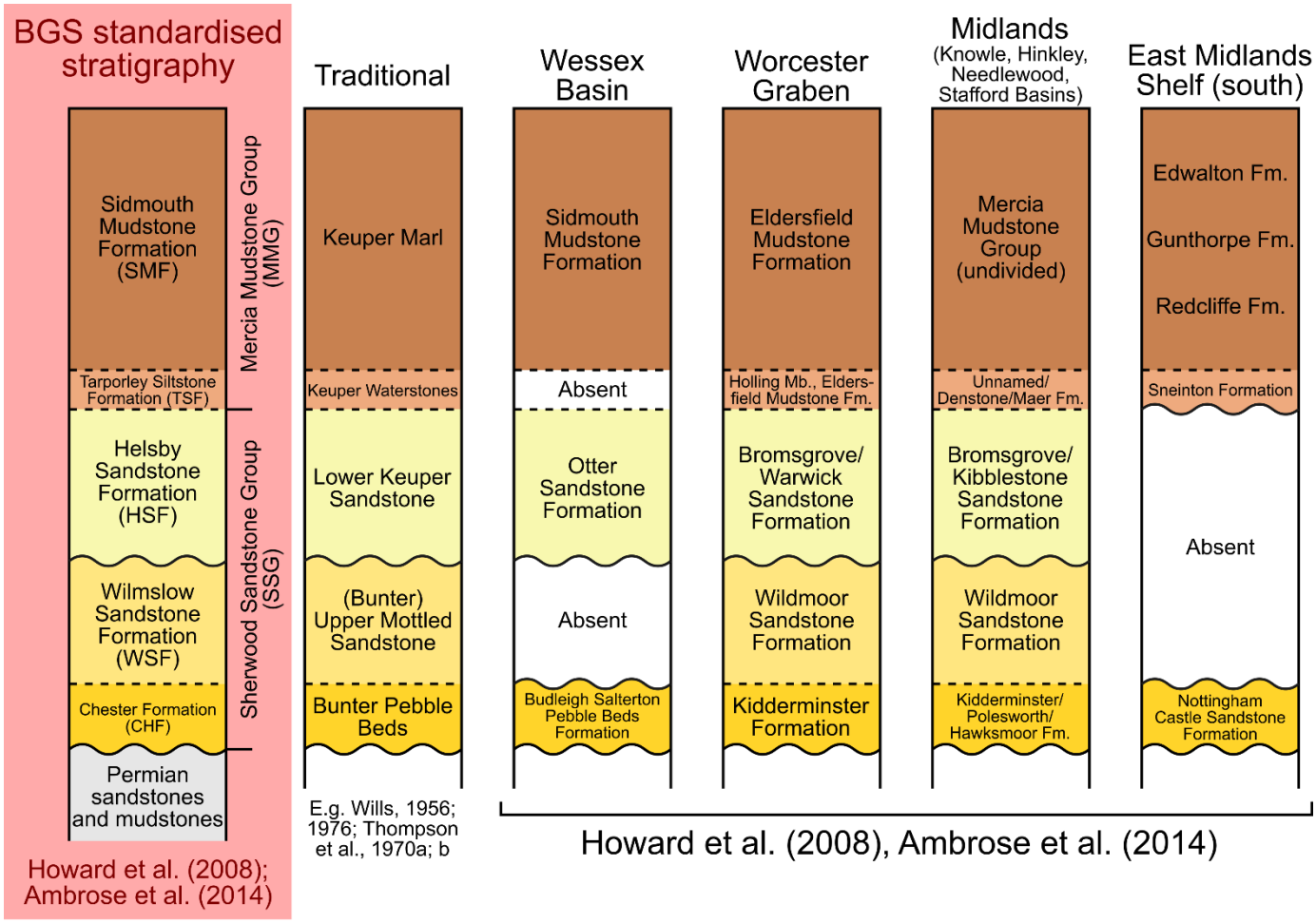
BGS standardised stratigraphy
Sidmouth Mudstone Formation (SMF)
Tarporley Siltstone Formation (TSF)
Helsby Sandstone Formation (HSF)
Wilmslow Sandstone Formation (WSF)
Chester Formation (CHF)
Permian sandstones and mudstones
Mercia Mudstone Group (MMG)
Sherwood Sandstone Group (SSG)
Howard et al. (2008); Ambrose et al. (2014)
Traditional
Keuper Marl
Keuper Waterstones
Lower Keuper Sandstone
(Bunter) Upper Mottled Sandstone
Bunter Pebble Beds
E.g. Wills, 1956; 1976; Thompson et al., 1970a; b
Wessex Basin
Sidmouth Mudstone Formation
Absent
Otter Sandstone Formation
Absent
Budleigh Salterton Pebble Beds Formation
Worcester Graben
Eldersfield Mudstone Formation
Holling Mb., Eldersfield Mudstone Fm.
Bromsgrove/ Warwick Sandstone Formation
Wildmoor Sandstone Formation
Kidderminster Formation
Midlands (Knowle, Hinkley, Needlewood, Stafford Basins)
Mercia Mudstone Group (undivided)
Unnamed/ Denstone/Maer Fm.
Bromsgrove/ Kibblestone Sandstone Formation
Wildmoor Sandstone Formation
Kidderminster/ Polesworth/ Hawksmoor Fm.
East Midlands Shelf (south)
Edwalton Fm.
Gunthorpe Fm.
Redcliffe Fm.
Sneinton Formation
Absent
Nottingham Castle Sandstone Formation
Howard et al. (2008), Ambrose et al. (2014)

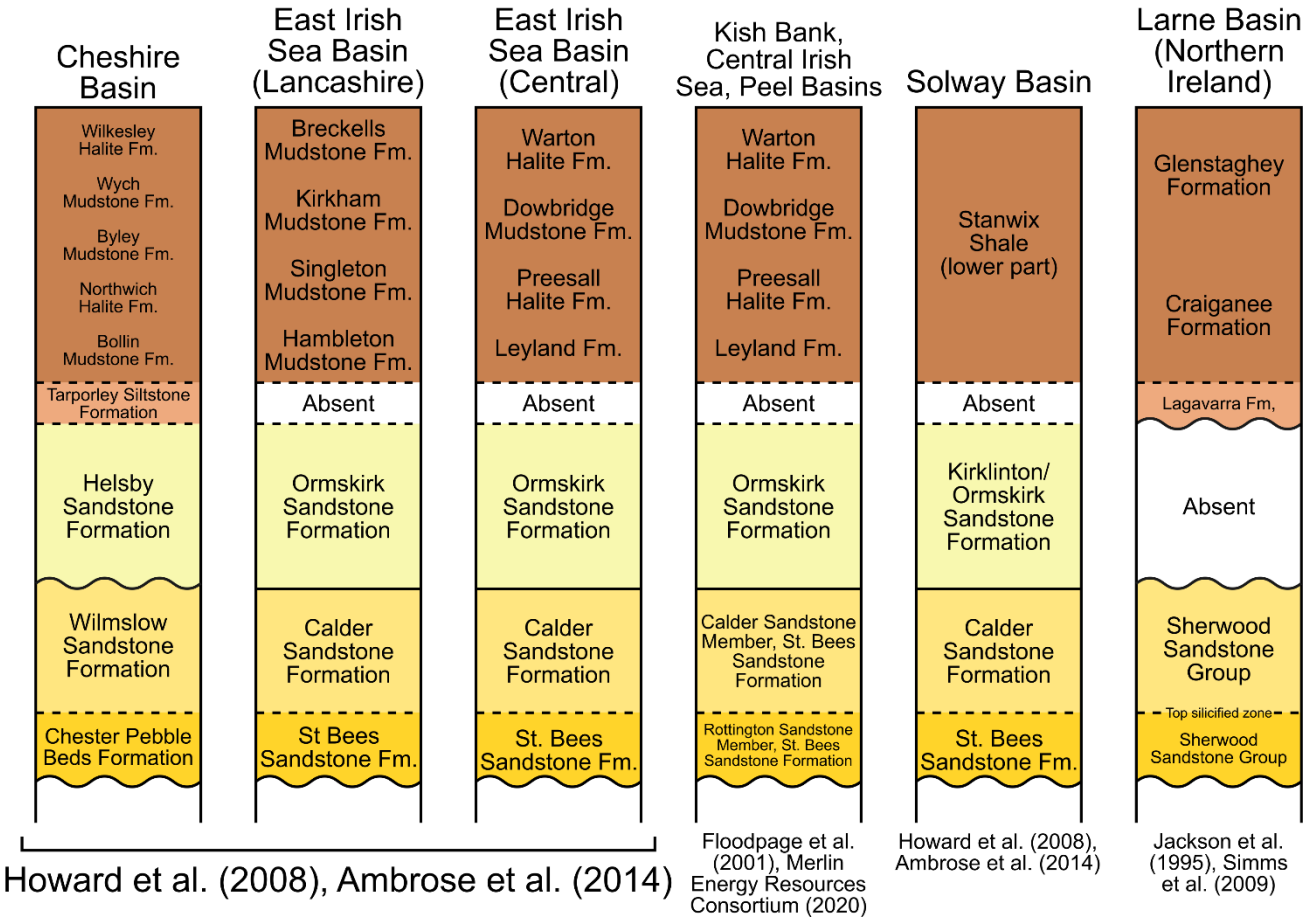
Cheshire Basin
Wilkesley Halite Fm.
Wych Mudstone Fm.
Byley Mudstone Fm.
Northwich Halite Fm.
Bollin Mudstone Fm.
Tarporley Siltstone Formation
Helsby Sandstone Formation
Wilmslow Sandstone Formation
Chester Pebble Beds Formation
East Irish Sea Basin (Lancashire)
Breckells Mudstone Fm.
Kirkham Mudstone Fm.
Singleton Mudstone Fm.
Hambleton Mudstone Fm.
Absent
Ormskirk Sandstone Formation
Calder Sandstone Formation
St Bees Sandstone Fm.
East Irish Sea Basin (Central)
Warton Halite Fm.
Dowbridge Mudstone Fm.
Preesall Halite Fm.
Leyland Fm.
Absent
Ormskirk Sandstone Formation
Calder Sandstone Formation
St. Bees Sandstone Fm.
Howard et al. (2008), Ambrose et al. (2014)
Kish Bank, Central Irish Sea, Peel Basins
Warton Halite Fm.
Dowbridge Mudstone Fm.
Preesall Halite Fm.
Leyland Fm.
Absent
Ormskirk Sandstone Formation
Calder Sandstone Member, St. Bees Sandstone Formation
Rottington Sandstone Member, St. Bees Sandstone Formation
Floodpage et al. (2001), Merlin Energy Resources Consortium (2020)
Solway Basin
Stanwix Shale (lower part)
Absent
Kirklinton/ Ormskirk Sandstone Formation
Calder Sandstone Formation
St. Bees Sandstone Fm.
Howard et al. (2008), Ambrose et al. (2014)
Larne Basin (Northern Ireland)
Glenstaghey Formation
Craiganee Formation
Lagavarra Fm,
Absent
Sherwood Sandstone Group
Top silicified zone
Sherwood Sandstone Group
Jackson et al. (1995), Simms et al. (2009)

Figure 2: Commonly used regional lithostratigraphic terms for the Sherwood Sandstone Group and Mercia Mudstone Group correlated to the BGS revised, standardised stratigraphy in Britain. See Ambrose et al. (2014) and Howard et al. (2008) for a comprehensive review of SSG and MMG regional terminology, respectively.

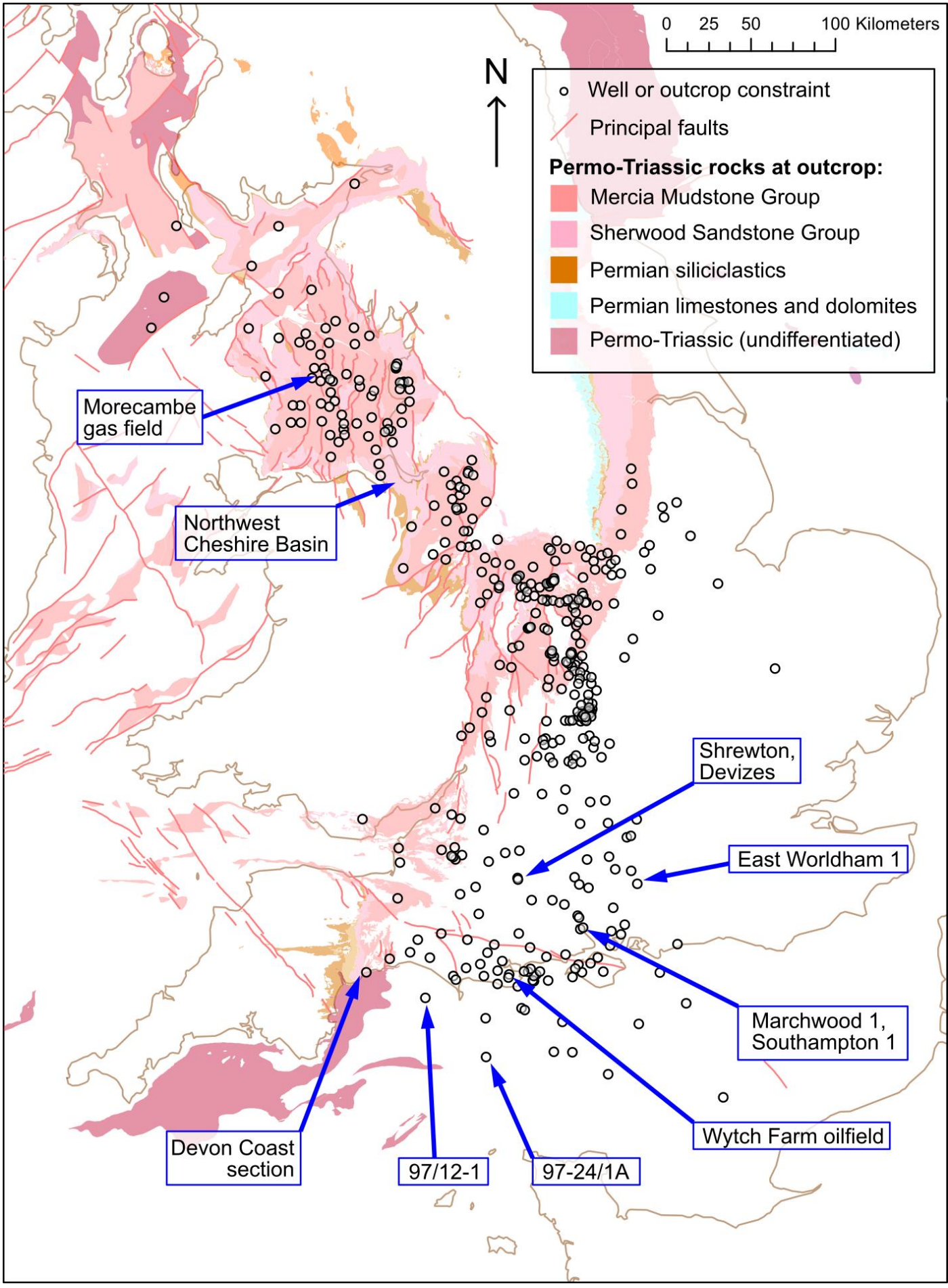
0 25 50 100 Kilometers
N
Well or outcrop constraint
Principal faults
Permo-Triassic rocks at outcrop:
Mercia Mudstone Group
Sherwood Sandstone Group
Permian siliciclastics
Permian limestones and dolomites
Permo-Triassic (undifferentiated)
Morecambe gas field
Northwest Cheshire Basin
Shrewton, Devizes
East Worldham 1
Marchwood 1, Southampton 1
Wytch Farm oilfield
Devon Coast section
97/12-1
97-24/1A

1635

Figure 3: Data framework composed of analysed boreholes and outcrops, overlaid on Permo-Triassic outcrop geology and structure of the British Isles. Labelled locations are mentioned in the text. Geological Map Data BGS © UKRI 2025

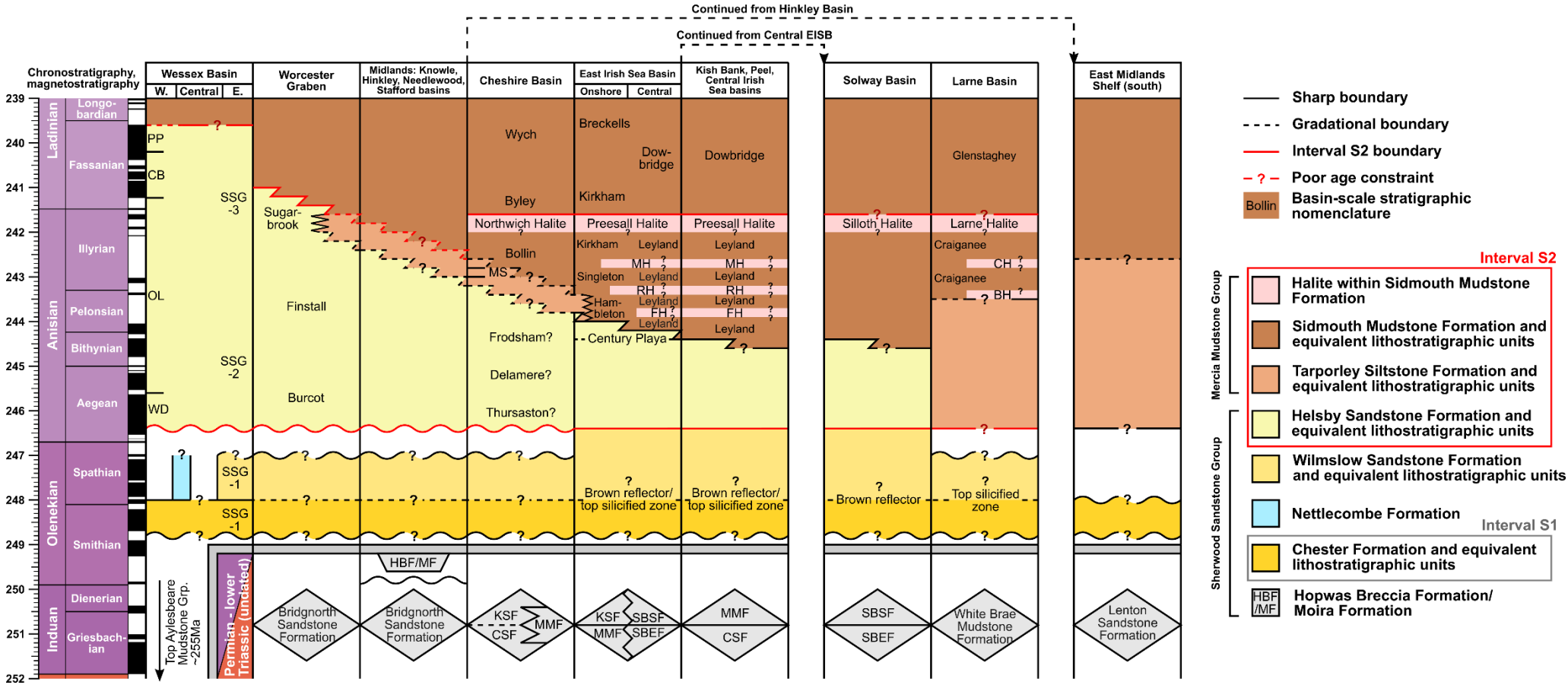
Continued from Hinkley Basin
Continued from Central EISB
Chronostratigraphy, magnetostratigraphy
Wessex Basin
W.
Central
E.
Worcester Graben
Midlands: Knowle, Hinkley, Needlewood, Stafford basins
Cheshire Basin
East Irish Sea Basin
Onshore
Central
Kish Bank, Peel, Central Irish Sea basins
Solway Basin
Larne Basin
East Midlands Shelf (south)
239
240
241
242
243
244
245
246
247
248
249
250
251
252
Ladinian
Anisian
Olenekian
Induan
Longo-bardian
Fassanian
Illyrian
Pelonsian
Bithynian
Aegean
Spathian
Smithian
Dienerian
Griesbach-ian
PP
CB
OL
WD
SSG -3
SSG -2
SSG -1
SSG -1
Sugar-brook
Finstall
Burcot
Wych
Byley
Northwich Halite
Bollin
MS
Frodsham?
Delamere?
Thursaston?
Breckells
Dow-bridge
Kirkham
Preesall Halite
Kirkham
Leyland
MH
Singleton
Leyland
RH
Ham-bleton
Leyland
FH
Leyland
Century Playa
Brown reflector/ top silicified zone
Dowbridge
Preesall Halite
Leyland
MH
Leyland
RH
Leyland
FH
Leyland
Brown reflector/ top silicified zone
Silloth Halite
Brown reflector
Glenstaghey
Larne Halite
Craiganee
CH
Craiganee
BH
Top silicified zone
Lenton Sandstone Formation
Top Aylesbeare Mudstone Grp. ~255Ma
Permian - lower Triassic (undated)
HBF/MF
Bridgnorth Sandstone Formation
Bridgnorth Sandstone Formation
KSF
CSF
MMF
KSF
MMF
SBSF
SBEF
MMF
CSF
SBSF
SBEF
White Brae Mudstone Formation
Sharp boundary
Gradational boundary
Interval S2 boundary
Poor age constraint
Bollin
Basin-scale stratigraphic nomenclature
Interval S2
Mercia Mudstone Group
Halite within Sidmouth Mudstone Formation
Sidmouth Mudstone Formation and equivalent lithostratigraphic units
Tarporley Siltstone Formation and equivalent lithostratigraphic units
Sherwood Sandstone Group
Helsby Sandstone Formation and equivalent lithostratigraphic units
Wilmslow Sandstone Formation and equivalent lithostratigraphic units
Nettlecombe Formation
Interval S1
Chester Formation and equivalent lithostratigraphic units
HBF /MF
Hopwas Breccia Formation/ Moira Formation

Figure 4: Integrated lithostratigraphic and chronostratigraphic correlation for the Permian to middle Triassic System in the British Isles, including undated Permo-Triassic units, the Sherwood Sandstone Group and lower Mercia Mudstone Group. Basins are ordered from southeast to northwest. Chronostratigraphic and magnetostratigraphic timescale adapted from Ogg et al. (2020). PP: Pennington Point Member, CB: Chiselbury Bay Member, OL: Otterton Ledge Member, WD: West Down Member, MS: Malpas Sandstone Member, MH: Mythrop Halite Member, RH: Rossall Halite Member, FH: Fylde Halite Member, CH: Carnduff Halite Member, BH: Ballybolley Halite Member, KS: Kinnerton Sandstone Formation, MMF: Manchester Marls Formation, CSF: Collyhurst Sandstone Formation, SBSF: St Bees Shale Formation, SBEF: St Bees Evaporites Formation

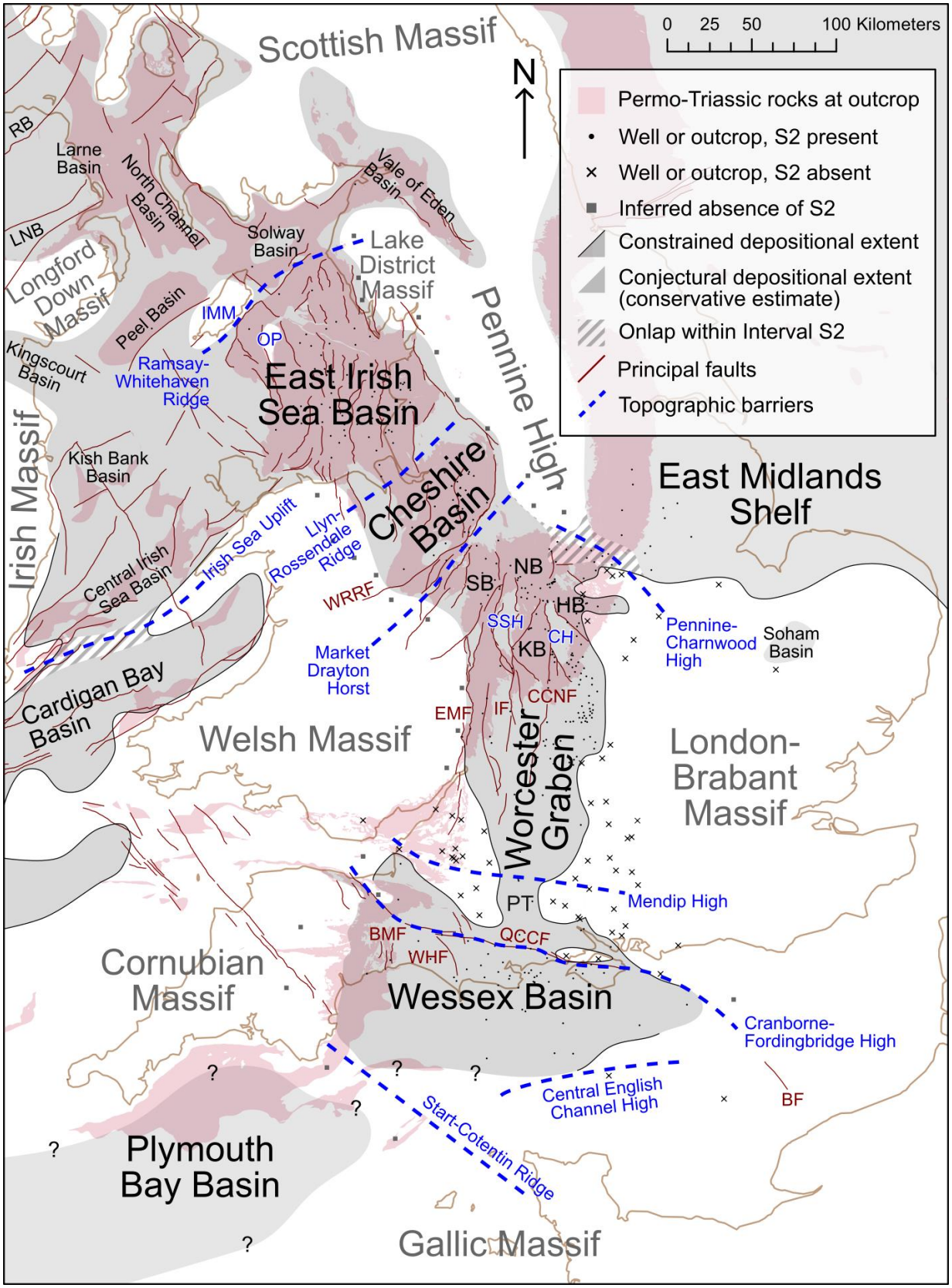

Figure 5: Structural and palaeogeographic setting during Interval S2 (middle Triassic) in the British Isles. Depositional extents outside geologically constrained areas from Jackson et al. (1995), Dunford et al. (2001); Simms et al. (2009) and McKie (2017). Structures adapted from DiGRock250k (2008; 2013) and Newell (2017a). BF: Bray Fault;

BMF: Beer-Musbury Fault; CH: Coventry Horst; CCNF: Clopton-Clapton-Northleach Fault; EMF: East Malvern Fault; HB: Hinkley Basin; IF: Inkerberrow Fault; IMM: Isle of Man Massif; KB: Knowle Basin; LNB: Lough Neagh Basin; NB: Needlewood Basin; OP: Ogham Platform; PT: Pewsey Trough; QCCF: Quantocks-Coker-Cranborne Fault; RB: Rathlin Basin; SB: Stafford Basin; SSH: South Staffordshire Horst; WRRF: Wem-Red Rock Fault. Geological Map Data BGS © UKRI 2025

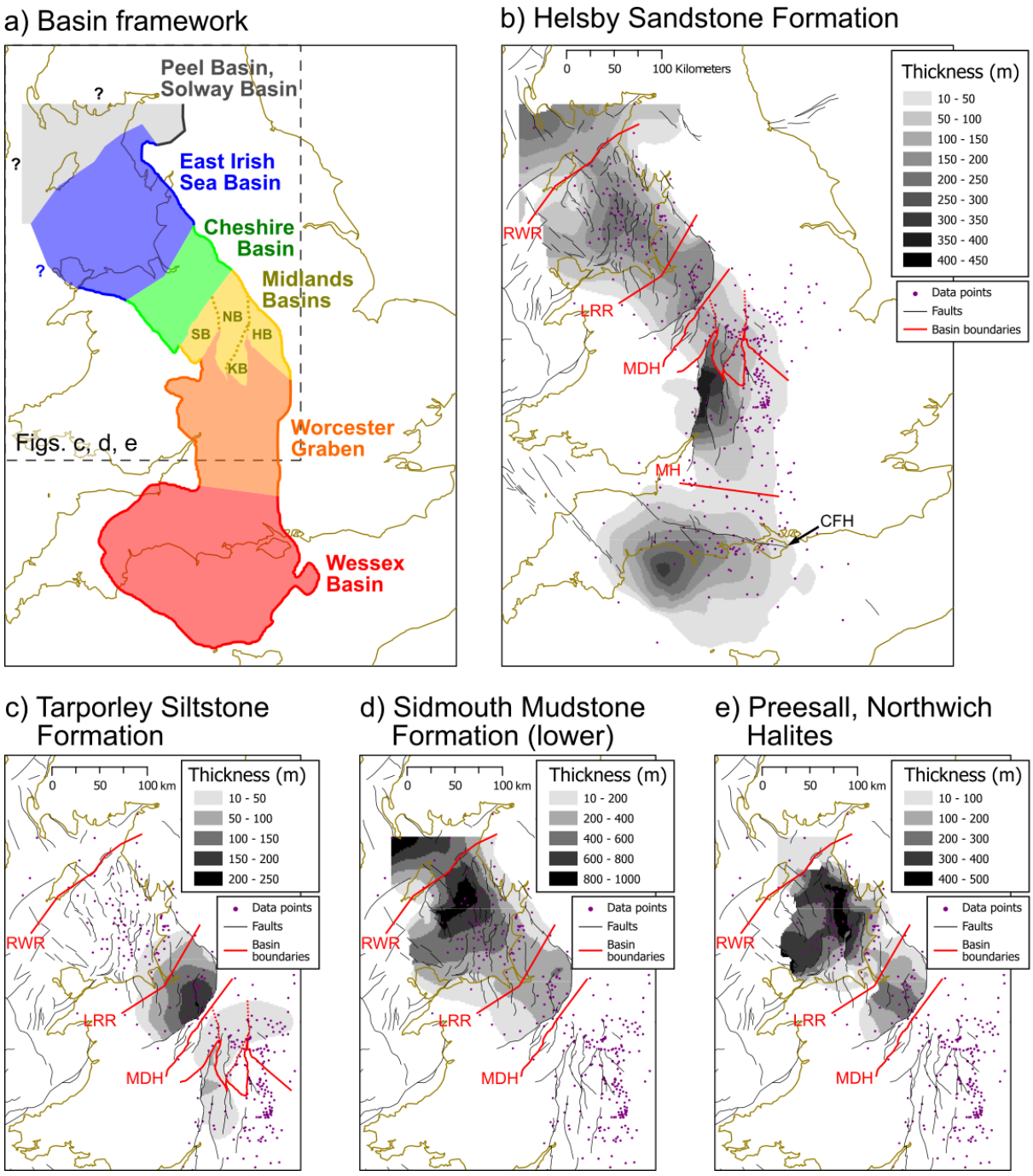

Figure 6: a) Basin configuration for isopach maps of the lithostratigraphic units of Interval S2. Isopach maps for the: **b)** Helsby Sandstone Formation **c)** Tarporley Siltstone Formation (MMG), **d)** Sidmouth Mudstone Formation (below but excluding the Preesall and Northwich Halites), **e)** Preesall and Northwich Halites. SB: Stafford Basin, NB: Needlewood Basin, HB: Hinkley Basin, KB: Knowle Basin. CFH: Cranborne-Fordingbridge High, MH: Mendip High, MDH: Market Drayton Horst, LRR: Llyn-Rossendale Ridge, RWR: Ramsay-Whitehaven Ridge.

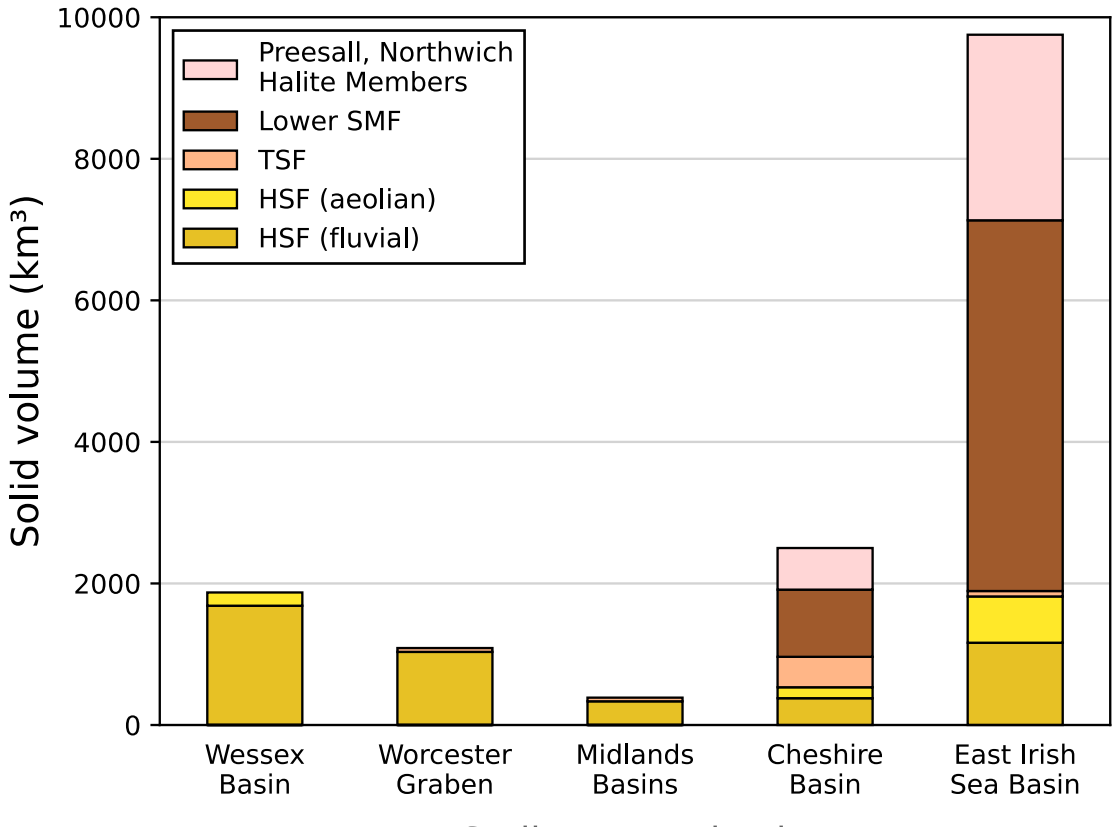

Figure 7: Solid rock (porosity removed) sediment volumes for the basins within Interval S2 (**fig. 2**), arranged downsystem (south to north) between the Wessex Basin and the EISB (**fig. 6**). Volumes are divided by respective lithostratigraphic units, and within the Helsby Sandstone Formation (HSF), by aeolian and fluvial deposits. TSF: Tarporley Siltstone Formation, SMF: Sidmouth Mudstone Formation.

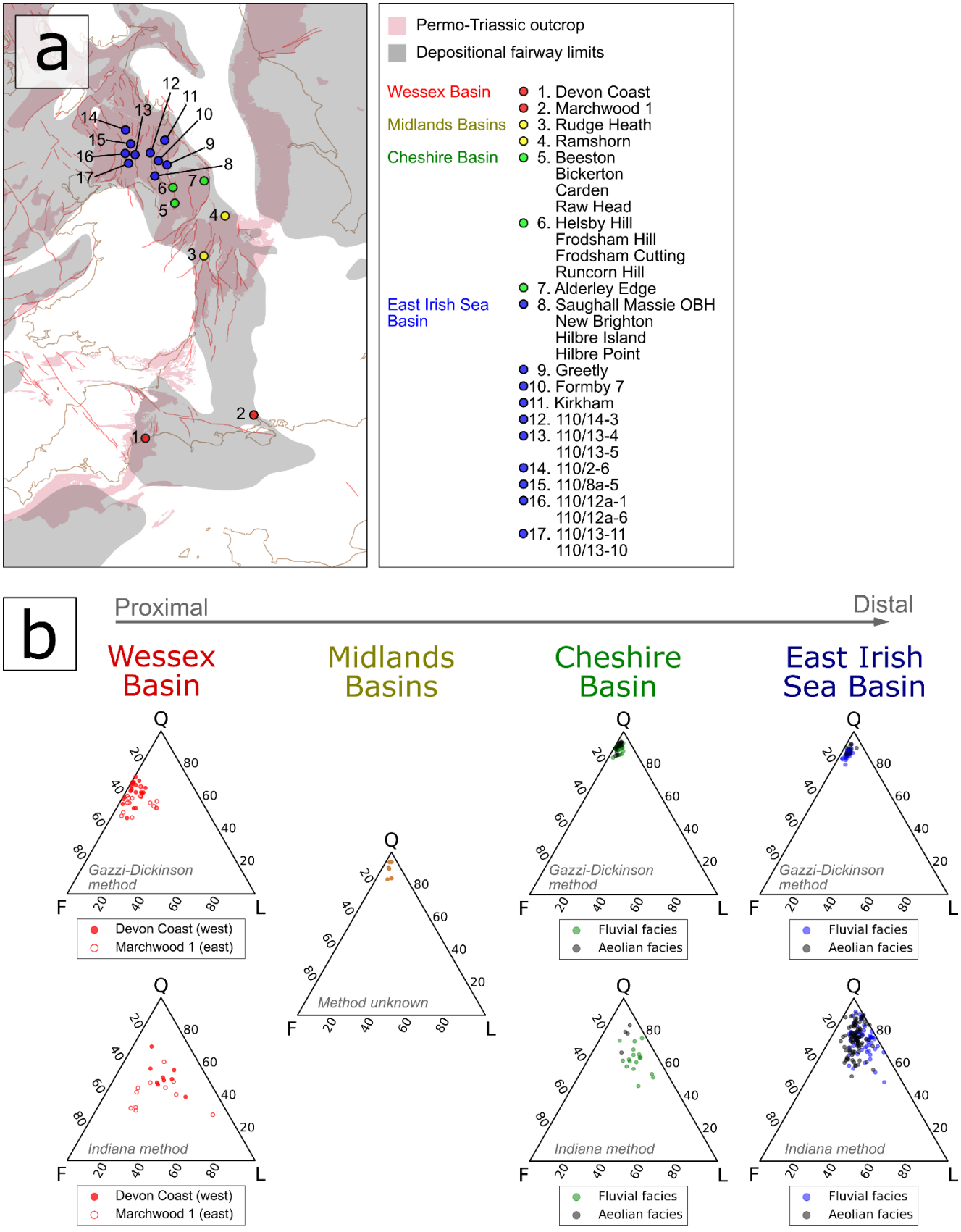

Figure 8: **a)** Map showing localities within the Helsby Sandstone Formation (HSF) where sandstone bulk petrographic data has been collected, divided by sedimentary basin (Knox et al., 1984; Burley, 1987; Ali, 1983; Chisholm et al., 1988; Scorgie et al., 2021; De

Sainz Simpson, 2022; Meadows, pers. comm). Geological Map Data BGS © UKRI 2025 **b)** Sandstone QFL plots for each basin area in the HSF, divided by point count method. Bulk mineralogical data are also divided between fluvial and aeolian deposits in the Cheshire Basin and EISB. Diagrams plotted using Ternary-Diagram (Yu9824, 2021).

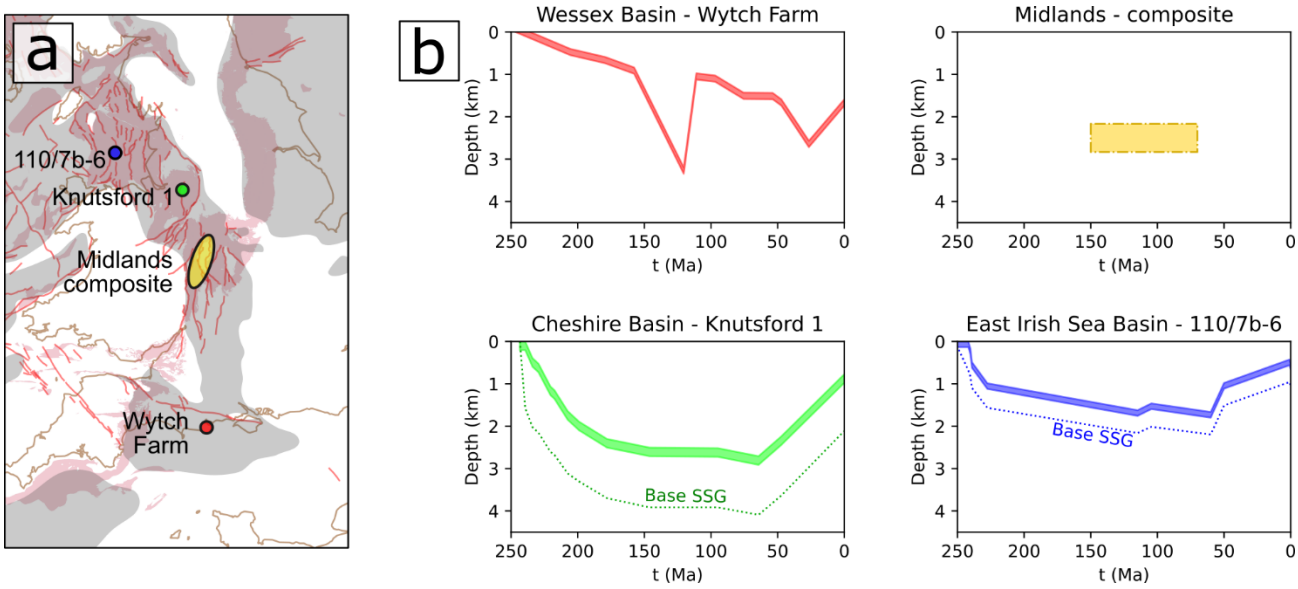

Figure 9: **a)** Map showing selected localities where burial histories for the Helsby Sandstone Formation (HSF) are reconstructed from vitrinite reflectance and apatite fission track analysis. Geological Map Data BGS © UKRI 2025 **b)** Representative burial histories for each basin, taken at the Wytch Farm oilfield for the Wessex Basin (Bray et al., 1998), a composite of wells in the western part of the Midlands Basins (Carter et al., 1995), well Knutsford 1 in the Cheshire Basin (Mikkelsen and Floodpage, 1997), and well 110/7b-6 in the EISB (Gent, 2006).

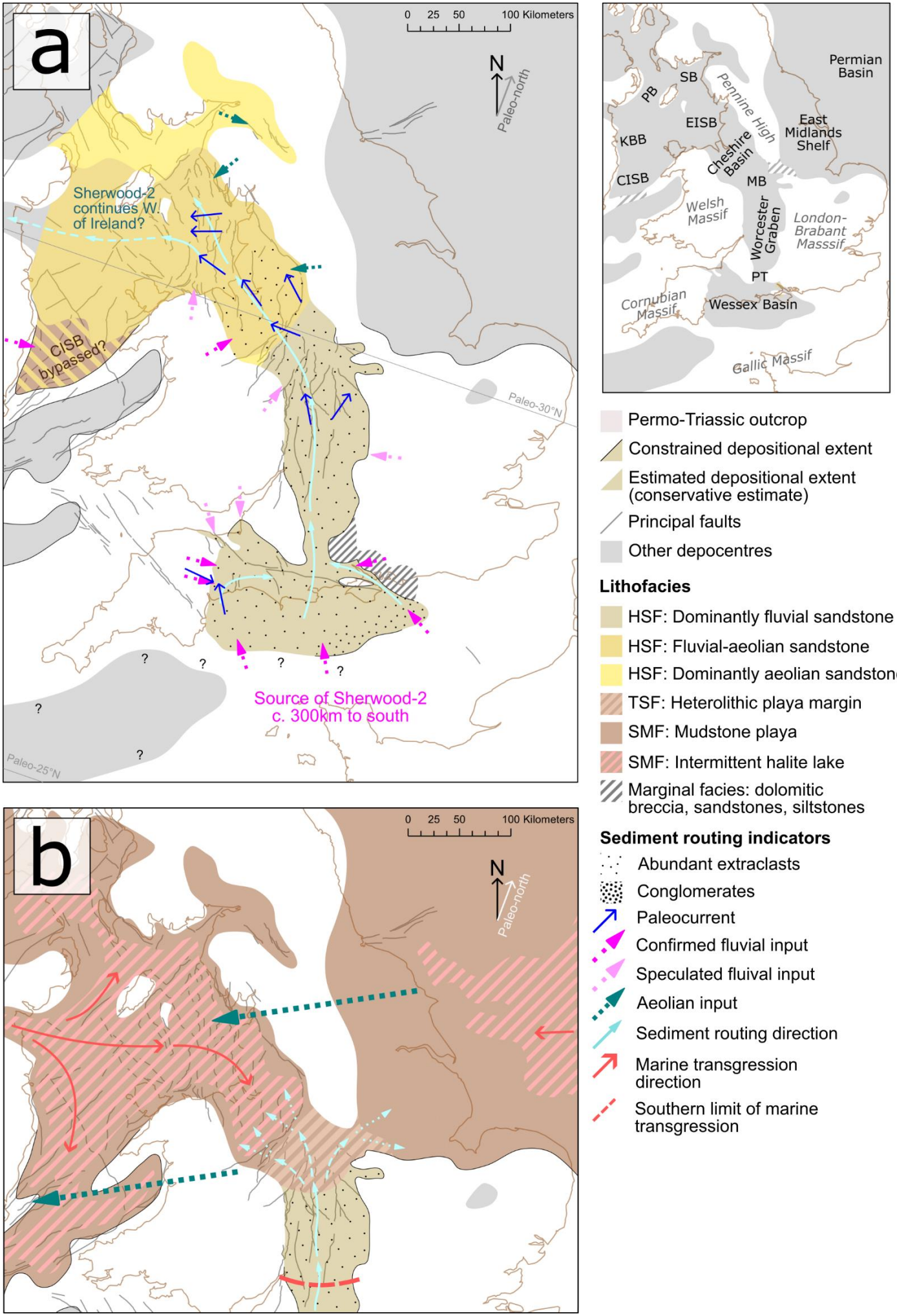
a
0 25 50 100 Kilometers
N
Paleo-north
Sherwood-2 continues W. of Ireland?
CISB bypassed?
Paleo-30°N
Source of Sherwood-2 c. 300km to south
Paleo-25°N
b
0 25 50 100 Kilometers
N
Paleo-north
Permian Basin
SB
PB
Pennine High
EISB
East Midlands Shelf
KBB
Cheshire Basin
CISB
MB
Welsh Massif
Worcester Graben
London-Brabant Masssif
PT
Cornubian Massif
Wessex Basin
Gallic Massif
Permo-Triassic outcrop
Constrained depositional extent
Estimated depositional extent (conservative estimate)
Principal faults
Other depocentres
Lithofacies
HSF: Dominantly fluvial sandstone
HSF: Fluvial-aeolian sandstone
HSF: Dominantly aeolian sandstone
TSF: Heterolithic playa margin
SMF: Mudstone playa
SMF: Intermittent halite lake
Marginal facies: dolomitic breccia, sandstones, siltstones
Sediment routing indicators
Abundant extraclasts
Conglomerates
Paleocurrent
Confirmed fluvial input
Speculated fluival input
Aeolian input
Sediment routing direction
Marine transgression direction
Southern limit of marine transgression

Figure 10: Depositional environments for **a)** the base of Interval S2 (**fig. 4,** Helsby Sandstone Formation, HSF), and **b)** the top of Interval S2 in the northern portion of the fairway (**fig. 4,** HSF, Tarporley Siltstone Formation (TSF), lower Sidmouth Mudstone Formation (SMF)). Also depicted are confirmed and speculated sediment inputs (Wills, 1956; 1976; Warrington and Ivimey-Cook, 1970; Smith and Edwards 1991; Jones and Ambrose, 1994; Mountney and Thompson, 2002; Tyrrell et al., 20125; Morton et al., 2013; 2016; Marsh et al., 2022), representative palaeocurrent measurements (Thompson, 1970b; Chisolm et al., 1988; Smith and Edwards, 1991; Old et al., 1987; 1991; Herries and Cowan, 1997; Newell, 2017) and first-order grain size changes. Palaeogeography and sediment fairway follows **fig. 5** and references therein. Palaeo-north and palaeolatitude from Dercourt et al. (2000). ESIB: East Irish Sea Basin, CISB: Central Irish Sea Basin, KBB: Kish Bank Basin, MB: Midlands Basins, PB: Peel Basin, PT: Pewsey Trough, SB: Solway Basin. **(a, b)** Geological Map Data BGS © UKRI 2025

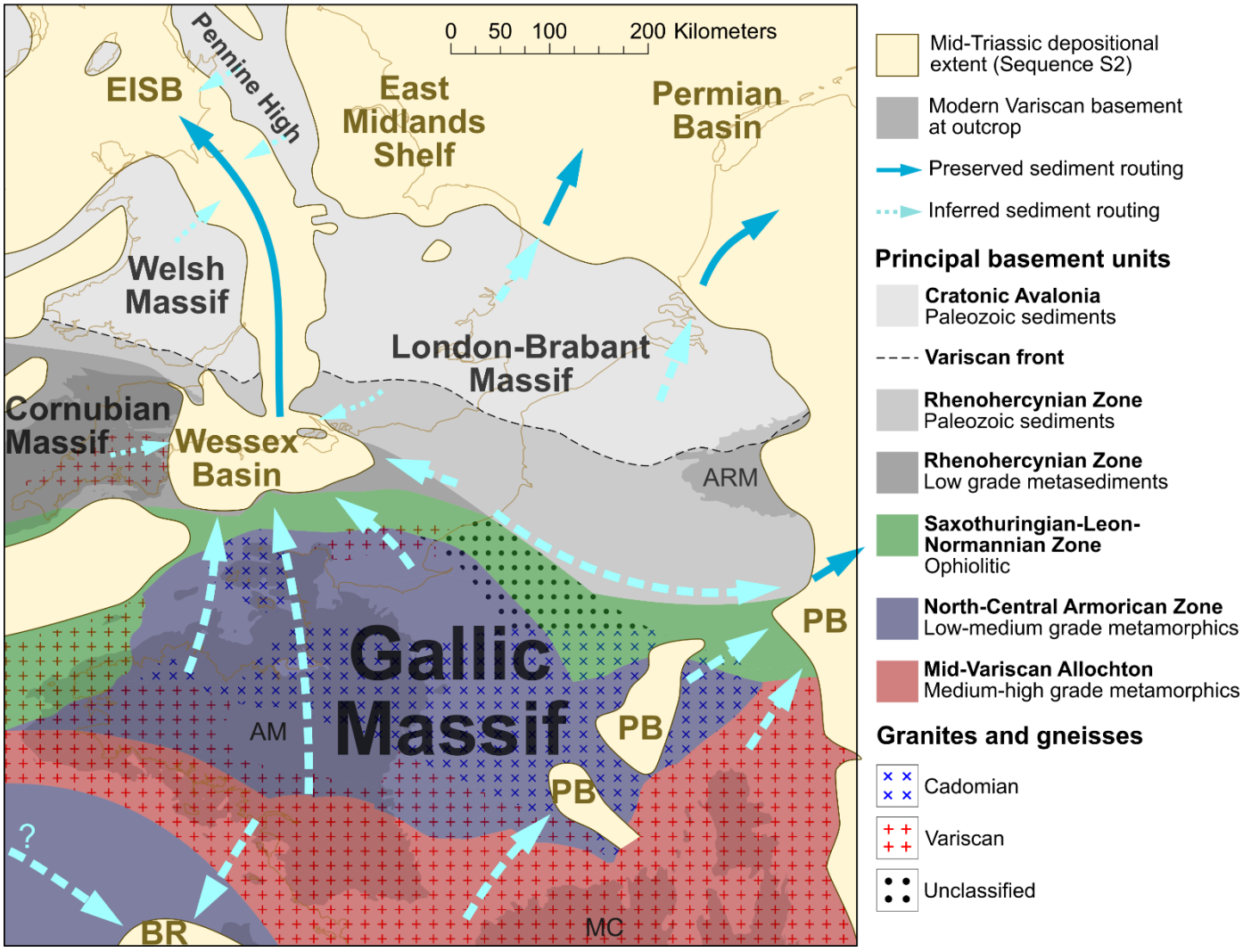

Figure 11: Triassic sedimentary basins and sediment routing in northwest Europe superimposed on a map of first-order Variscan tectonic units. UK basins from **fig. 5,** and references therein. Other basins from Bourquin et al. (2006), McKie et al. (2017), and Ceccetti et al. (2024). Basin and sediment routing configuration is portrayed for the mid-Anisian. AM: Armorican Massif, ARM: Ardennes-Rhenish Massif MC: Massif Central. BR: Biscay Rift, PB: Paris Basin. Basement lithologies for continental Europe adapted from Megnien (1980), Baptiste (2016), Laurent et al. (2021) and Catalán et al. (2021). Basement lithologies for the English Channel area adapted from Hamblin et al. (1992), Shail and Leveridge (2009) and Baptiste (2016). Basement lithologies for the UK adapted from Shail and Leveridge (2009); Butler (2018), and Pullan and Donato (2022)